NASA Technical Memorandum 101612

PRELIMINARY DESIGN OF A LARGE TETRAHEDRAL TRUSS/HEXAGONAL HEATSHIELD PANEL AEROBRAKE

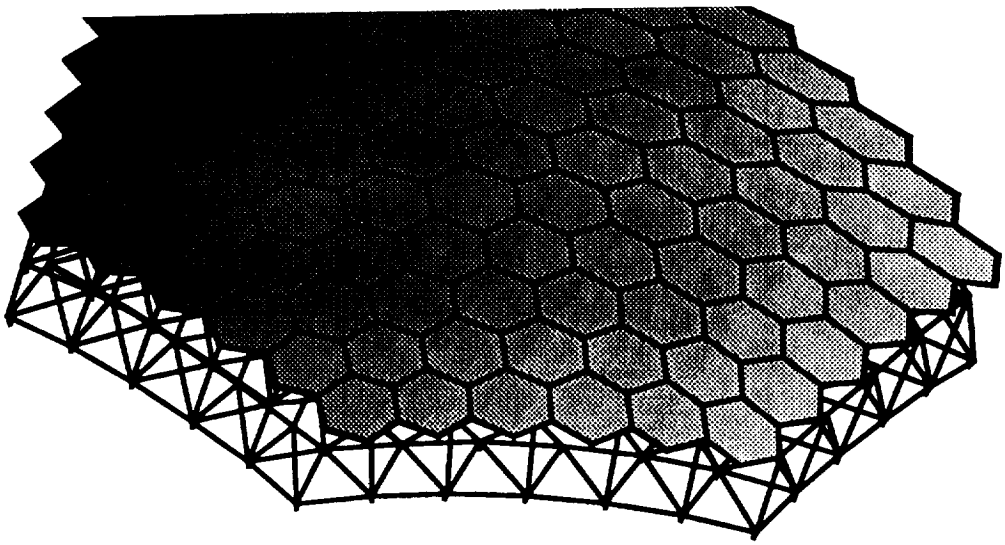

John T. Dorsey and Martin M. Mikulas, Jr.

SEPTEMBER 1989

NASA

National Aeronautics and Space Administration

Langley Research Center
Hampton, Virginia 23665

PRELIMINARY DESIGN OF A LARGE TETRAHEDRAL TRUSS/HEXAGONAL HEATSHIELD PANEL AEROBRAKE

John T. Dorsey and Martin M. Mikulas, Jr.

INTRODUCTION

A great deal of interest has recently been expressed in the area of manned exploration of the solar system, especially a manned mission to Mars (reference 1). Preliminary studies have determined that a manned sprint mission to Mars will require two large vehicles (reference 2); an unmanned cargo vehicle with a mass of several million pounds, and a manned sprint vehicle (also massive and containing a large amount of pressurized habitation volume). These vehicles will be too large and massive to be placed in orbit by a single launch of the Space Shuttle, or even a Heavy Lift Launch Vehicle, and some on-orbit assembly and construction will be required (reference 3).

A large portion of the mass for both Mars vehicles is the propellant required for propulsive braking both at Mars and on Earth return. Aerobraking uses aerodynamic drag forces rather than propellant burns to produce the velocity decrements required at Mars and Earth, and thus provides one of the most effective ways to reduce the size and mass of Mars mission vehicles (reference 4). Preliminary estimates show that the aerobrake required for a manned Mars vehicle will be on the order of 90 to 120 feet in diameter and as a result, the aerobrake will have to be assembled on orbit. In addition, the aerobrake will be a heavily loaded structure since the pressure on the aerobrake during Martian atmospheric entry results in vehicle decelerations of up to 6 g's. The large size and heavy loads present both structural design and assembly challenges for the aerobrake, challenges which are new and different from lightly loaded and stiffness designed large space structures currently being considered (such as antennas, and Space Station Freedom). In order for the aerobrake to be viable from a mission standpoint, it must; be lightweight, have minimum packaged volume for shipment to Low Earth Orbit, and incorporate design-for-construction techniques which emphasize ease of on-orbit assembly.

This paper introduces an aerobrake structural concept consisting of two primary components; 1) a lightweight erectable tetrahedral support truss, and 2) sandwich hexagonal heatshield panels which, when attached to the truss, form a continuous aerobraking surface which is impermeable to hot gas flow through its thickness. Since trusses are designed specifically to have members which carry all loads in tension or compression, trusses represent the most efficient structural form (see reference 3). Thus, the concept presented in this paper can potentially result in very lightweight aerobrake designs. In addition, aerobrake support truss components (struts and nodes) can be transported to orbit disassembled, allowing for efficient packaging in a minimum volume. Once in orbit, the truss can be assembled either manually (reference 5) or telerobotically (reference 6). The heatshield panels, with diameters sized by the payload envelope of the launch vehicle, can also be assembled to the truss either manually or telerobotically.

One objective of this paper is to develop generic finite element models and a general analysis procedure to design tetrahedral truss/hexagonal heatshield panel aerobrakes. A second objective is to determine the values of the aerobrake design parameters which minimize mass and packaging volume for a 120 foot diameter aerobrake, allowing its design viability to be assessed. A third objective is to determine the sensitivity of the total aerobrake mass and volume, as well as its structural performance, to variations in design parameters. The fourth and final objective is to calculate the support truss strut loads, and consequently, the strut sizes, to serve as input for designing heavily loaded truss joints and aerobrake assembly studies.

NOMENCLATURE

a	panel diameter, in
A	area, in^2
A_{11}, A_{12}, A_{22}, A_{66}	laminate extensional stiffnesses, lbf/in
α	panel coefficient, see equation (17)
C_1	local buckling constant, see equation (9)
d	diameter, in
D	panel bending stiffness, in-lbf
E	Young's modulus, lbf/in^2
ε, γ	laminate strains, in/in
G	shear modulus, lbf/in^2
I	cross-sectional moment of inertia, in^4
K	knockdown factor
L	length, in
L/D	lift to drag ratio
M	mass, lbm
N	force resultants acting on a laminate, lbf/in
N_R	number of rings in the support truss
ν	Poisson's ratio
P	load, lbf
q	pressure loading, lbf/in^2
R	radius, in
ρ	material density, lbm/in^3
σ	stress, lbf/in^2
t	thickness, in
w_{max}	maximum deflection, in

x	radial distance from aerobrake or panel center, in

Subscripts:

AB	aerobrake
APP	applied
c	core
co	cutoff value
EB	Euler buckling
eff	effective
f	face sheet
HP	hexagonal panel
LB	local cylinder wall buckling
max	maximum allowable stress, or quantity resulting from its use
mg	minimum gauge
mm	minimum mass
s	strut
tfmg	minimum gauge face sheet thickness
θ	layup direction of truss strut walls, deg
x, y	laminate axes (x is along the strut longitudinal axis)
1, 2	laminae axes (1 is in the fiber direction)

Superscripts:

0	laminate middle surface

CONCEPT DESCRIPTION

The aerobrake structural concept being introduced in this paper consists of two major components; a tetrahedral support truss and a heatshield composed of individual hexagonal panels (see figure 1). The heatshield panels are attached to the truss nodes at three of their vertices as shown in the figure, and cover the entire truss to form a continuous surface which is impermeable to hot gas flow. The current concept has been applied to aerobrakes with relatively low lift to drag ratios ($0 \leq L/D \leq 0.5$) and shapes which are either spherical or parabolic.

The strut arrangement in a tetrahedral truss results in upper and lower surfaces of triangular networks separated by core struts forming tetrahedrons. The geometry and structural properties of tetrahedral trusses are discussed at length in reference 7. One possible tetrahedral truss top surface planform is shown in figure 2. The struts in this particular arrangement can conveniently be grouped into rings, as defined in the figure. For a flat truss, all struts have equal length, with the length determined by dividing the truss diameter,d_{AB}, by twice the number of rings, N_R. Truss joints are

located at the points where the truss struts intersect and the struts are assumed to have no moment carrying capability (ie. are pinned) at these locations. The struts are made of graphite epoxy and their cross section is a thin annulus as shown in figure 2. The strut walls are constructed from alternating $\pm \theta$ plies and the resulting lay-up is symmetric about the strut wall center line.

An individual hexagonal heatshield panel is shown superimposed on a triangular face of the tetrahedral support truss in figure 3. The panel diameter is measured across the points of the hexagon with the diameter fixed by the underlying support truss strut length. In order to efficiently resist bending, the panel uses sandwich construction consisting of an aluminum honeycomb core and graphite epoxy face sheets. The aerobrake thermal protection system (which could be an ablator or reusable ceramic tiles, depending on the application) is applied to one face of the structural panel to complete the heatshield system.

DESIGN AND SIZING EQUATIONS

As a vehicle using aerobraking enters a planet's atmosphere, an applied pressure results over the aerobrake surface which decelerates the vehicle. Current studies for manned Mars mission vehicles indicate that aerobraking can result in maximum decelerations of up to 6 g's. This load will be used in subsequent aerobrake structural design studies. The best aerobrake design is one which is strong enough to survive atmospheric entry, large enough to protect the attached spacecraft, and yet, has the minimum mass and packaging volume for transportation to Low Earth orbit. The aerobrake design can be separated into two problems; the support truss structure, and the heatshield panels (see figure 4). The support truss must be designed to distribute the aerodynamic pressure force from the heatshield to the spacecraft attachment points. The heatshield panels will span fairly large distances, and because of aerodynamic and thermal protection system deflection requirements, are not allowed to deform substantially under load. Thus the panels will be designed according to deflection requirements. For both problems, the pressure distribution over the aerobrake is assumed to be constant and proportional to deceleration rate. A major assumption made to simplify the derivations of the support truss and hexagonal panel design equations, is that the aerobrake has no curvature. This assumption is validated for values of $L/D \leq 0.5$ in the appendix.

The total nodal forces applied to the support truss equal the surface pressure times the total area of the support truss hexagonal planform. This force also equals the spacecraft mass (total vehicle mass - aerobrake mass) multiplied by the deceleration loading in g's. The nodal forces are applied to the top truss face in the direction shown in figure 4. The strut loads resulting from the applied forces are then used to design and size the support truss struts. Deceleration forces must be transmitted from the aerobrake structure to the attached spacecraft through discrete attachment points. For this study, these attachments are represented by simple support constraints applied to selected nodes on the back surface of the truss. These truss load points are located on a circle which has a radius of one half of the aerobrake total radius, and either 3, 4, or 6 points are used in the patterns shown in figure 5. These particular points are chosen because they are common to all four of the support truss geometries (2, 4, 6, and 8 rings) being considered.

A special support condition is obtained by using a support truss which has a triangle rather than a node at the truss center. Loading the truss at the three nodes of this central triangle is considered a single load point for a truss with a large number of rings. This might represent how a thruster would be attached to the center of a large tetrahedral truss for example.

A uniform pressure loading is applied to the hexagonal heatshield panel in the direction shown in figure 4. The panel is simply supported at three of its verticies as shown in figure 3, where the simply support condition represents the attachment between the panel and the underlying support truss.

Support Truss Struts

In this section, the detailed strut design procedure is described. Strut local wall buckling and Euler buckling criteria are used to select the strut wall layup which results in a minimum mass strut, and also to size the struts. In addition, equations are developed to design struts with minimum gauge wall thickness and maximum allowable stress constraints.

For a strut with a thin annular cross section, the area (A_s) and the moment of inertia (I_s) can be approximated by

$$A_s = 2 \pi R_s t_s \tag{1}$$

$$I_s = \pi R_s^3 t_s \tag{2}$$

where R_s is the strut radius and t_s is the strut wall thickness.

The strut walls are composite laminates which are symmetric about the middle surface. The general constitutive equations for this specially orthotropic laminate are (see reference 8)

$$\begin{Bmatrix} N_x \\ N_y \\ N_{xy} \end{Bmatrix} = \begin{bmatrix} A_{11} & A_{12} & 0 \\ A_{12} & A_{22} & 0 \\ 0 & 0 & A_{66} \end{bmatrix} \begin{Bmatrix} \varepsilon_x^0 \\ \varepsilon_y^0 \\ \gamma_{xy}^0 \end{Bmatrix} \tag{3}$$

where N_x, N_y, and N_{xy} are the force resultants acting on the laminate, A_{ij} are the laminate extensional stiffnesses, and ε_x^0, ε_y^0, and γ_{xy}^0 are middle surface strains. The equation for N_y in (3) can be solved to give

$$\varepsilon_y^0 = \frac{N_y - A_{12} \varepsilon_x^0}{A_{22}} \tag{4}$$

Substituting (4) into the equation for Nx in (3) and dividing by the thickness gives the following expression for the axial stress in a strut

$$\frac{N_x}{t_s} = \frac{1}{t_s}\left(A_{11} - \frac{A_{12}^2}{A_{22}}\right)\varepsilon_x^0 + \frac{A_{12}}{A_{22}}\frac{N_y}{t_s} \tag{5}$$

When only an axial load, N_x, is applied to the strut, (5) reduces to

$$\frac{N_x}{t_s} = \frac{1}{t_s}\left(A_{11} - \frac{A_{12}^2}{A_{22}}\right)\varepsilon_x^0 \tag{6}$$

Comparing (6) with the isotropic stress-strain relationship

$$\sigma_x = E_{eff}\,\varepsilon_x \tag{7}$$

results in the following definition for the strut effective Young's modulus

$$E_{eff} = \frac{1}{t_s}\left(A_{11} - \frac{A_{12}^2}{A_{22}}\right) \tag{8}$$

The local wall buckling stress for a imperfect, simply supported cylinder is (see reference 7)

$$\sigma_{LB} = K_{LB}\,C_1\,\frac{E_{eff}\,t_s}{R_s} \tag{9}$$

where K_{LB} is a knockdown factor associated with imperfections in the cylinder and C_1 is a function of the cylinder wall layup (equal to 0.6 for a isotropic cylinder). For a simply supported cylinder with multiple orthortropic layers, the local wall buckling stress, σ_{LB}, is found using equations developed in reference 9. For each different wall layup, σ_{LB} and the associated strut effective modulus, radius and wall thickness are substituted into equation (9) allowing the corresponding value of C_1 to be calculated. For this calculation, the cylinder is assumed to be perfect and thus $K_{LB} = 1$.

The Euler buckling stress for a simply supported strut is

$$\sigma_{EB} = \frac{K_{EB}\,\pi^2\,E_{eff}\,R_s^2}{2\,L_s^2} \tag{10}$$

where L_s is the strut length. K_{EB} is a knockdown factor used to account for load eccentricity and to limit the influence of bending stresses due to initial strut curvature. The axial stress in a strut resulting from the applied nodal loads is

$$\sigma_{APP} = \frac{P_s}{2\,\pi\,R_s\,t_s} \tag{11}$$

where Ps are the strut axial loads determined from the support truss finite element model.

For buckling critical struts, a minimum mass design is obtained when

$$\sigma_{LB} = \sigma_{EB} = \sigma_{APP} \tag{12}$$

Equating equations (9) and (11) gives the following expression for determining the wall thickness of a minimum mass strut

$$t_{s_{mm}} = \left[\frac{P_s}{2 \pi K_{LB} C_1 E_{eff}} \right]^{1/2} \tag{13}$$

Similarly, equating equations (10) and (11) gives the associated radius for a minimum mass strut

$$R_{s_{mm}} = \left[\frac{P_s L_s^2}{K_{EB} \pi^3 E_{eff} t_{s_{mm}}} \right]^{1/3} \tag{14}$$

For struts which are not designed for minimum mass, as long as $R_s / t_s \leq R_{s_{mm}} / t_{s_{mm}}$, the strut will not buckle locally for the design load.

The strut mass can be calculated from

$$M_s = 2 \pi \rho_s R_s t_s L_s \tag{15}$$

where ρ_s is the strut material density. For a minimum mass strut, the strut mass parameter, M_s / L_s^3, can be plotted as a function of the loading index, P_s / L_s^2, independent of strut dimensions (see reference 7).

In general, two other strut design conditions besides minimum mass must be addressed; minimum gauge thickness, and maximum allowable stress. For small values of compressive loading, P_s, the strut wall thickness determined by equation (13) may be less than the practical minimum gauge for the material being used. In this case, the strut minimum gauge thickness, $t_{s_{mg}}$, is used in place of the minimum mass strut thickness but equation (14) is still used to calculate the strut radius. Since the value of R_s/t_s obtained using the minimum gauge values for a particular strut load is less than the value of R_s/t_s for a minimum mass strut, the strut will still satisfy the local buckling criteria. The Euler buckling criteria will be satisfied since equation (14) is used to calculate the strut radius. For a strut designed using the minimum gauge thickness constraint, the strut mass depends on the thickness to length ratio, t_s / L_s, as well as on the loading index (see reference 7).

In general, the material ultimate strength will require that a maximum allowable stress, σ_{max}, not be exceeded in the strut. For large values of compressive loading however, a minimum mass strut design (which is based only on buckling criteria) will

result in a cross-sectional area which renders $\sigma_{APP} > \sigma_{max}$. Thus, the strut area required to reduce the applied stress to an acceptable level is obtained as follows: the strut radius resulting from the minimum mass calculation is retained, and a new strut thickness, which is larger than the value obtained from the minimum mass equation, is calculated according to

$$t_{s_{max}} = \frac{P_s}{2 \pi R_{s_{mm}} \sigma_{max}} \tag{16}$$

A strut designed with a radius from equation (14) and thickness from equation (16) has a larger moment of inertia, and a smaller value of R_s / t_s than a minimum mass design, ensuring that both the Euler and local buckling criteria are still met. Since a strut designed for maximum allowable stress has a particular amount of area, the mass parameter is only a function of the loading index and is independent of strut dimensions for individual values of σ_{max}.

Hexagonal Heatshield Panels

The heatshield panels are hexagonal in shape. In order to achieve high stiffness and low mass, a sandwich construction with a aluminum honeycomb core and graphite epoxy face sheets is used. For a panel subjected to a uniform pressure load, the maximum deflection occurs at the panel center and is

$$w_{max} = \alpha \frac{q\, a^4}{D_{HP}} \tag{17}$$

where q is the pressure loading, a is the panel diameter (measured between opposing verticies), and D_{HP} is the panel bending stiffness. The coefficient α, depends on both the panel boundary conditions and the panel geometry and is determined by numerical experiment using finite element analysis. The value of α does not depend on the panel stiffness parameter or diameter however. For a sandwich panel with a face sheet thickness t_f which is much less than the core thickness t_c, the bending stiffness can be approximated as (see reference 10)

$$D_{HP} = \frac{E_f\, t_f\, t_c^2}{2\,(1 - \nu_f^2)} \tag{18}$$

where E_f and ν_f are the Young's modulus and Poisson's ratio, respectively, of the graphite epoxy face sheet layup. The mass per unit area of the hexagonal panel is

$$(M / A)_{HP} = 2 \rho_f t_f + \rho_c t_c \tag{19}$$

where ρ_f and ρ_c are the densities of the face sheet and core materials respectively. Solving equation (17) for D_{HP} and substituting the result into equation (18) and then solving the resulting equation for t_f and substituting into equation (19) gives the hexagonal panel mass in terms of the core thickness

$$(M/A)_{HP} = \frac{4\,\alpha\,\rho_f\,q\,a^3\,(1-\nu_f^2)}{(w_{max}/a)\,E_f\,t_c^2} + \rho_c\,t_c \tag{20}$$

In this equation, the quantity, (w_{max}/a) is identified as a normalized panel maximum deflection criteria. The core thickness for a minimum mass hexagonal panel is found by solving the equation

$$\frac{\partial}{\partial t_c}(M/A)_{HP} = 0 \tag{21}$$

The resulting core thickness for a minimum mass panel is

$$t_{c_{mm}} = \left[8\,\alpha\,\frac{\rho_f}{\rho_c}\,\frac{(1-\nu_f^2)}{E_f}\,\frac{q\,a^3}{(w_{max}/a)}\right]^{1/3} \tag{22}$$

If equation (17) is solved for the panel stiffness, divided by α and compared to equation (22), minimum mass core thickness is seen to be a function of just the material properties and a panel stiffness parameter, defined as $\frac{q\,a^3}{(w_{max}/a)}$. Substituting equations (22) and (17) into (18) results in the following associated face sheet thickness for a minimum mass panel

$$t_{f_{mm}} = 0.25\,\frac{\rho_c}{\rho_f}\,t_{c_{mm}} \tag{23}$$

For a lightly loaded panel, the value of face sheet thickness determined by equation (23) may be less than the practical limit for the material being used. In this case it is helpful to define a cutoff value of the panel stiffness parameter, where values below the cutoff must be designed for face sheet minimum gauge thickness. Solving equation (17) for the panel stiffness and substituting into equation (18) gives the following expression for determining the panel stiffness parameter cutoff value for minimum gauge face sheets

$$\left[\frac{q\,a^3}{(w_{max}/a)}\right]_{co} = \frac{8}{\alpha}\,\frac{\left(\frac{\rho_f}{\rho_c}\right)^2 E_f}{(1-\nu_f^2)}\,t_{f_{mg}}^3 \tag{24}$$

where $t_{f_{mg}}$ is the face sheet minimum gauge thickness. The core thickness associated with a panel stiffness below the cutoff value (which requires the minimum gauge face sheet thickness) is given by

$$t_{c_{tfmg}} = \left[2\,\alpha\,\frac{(1-\nu_f^2)}{E_f\,t_{f_{mg}}}\,\frac{q\,a^3}{(w_{max}/a)}\right]^{1/2} \tag{25}$$

RESULTS AND DISCUSSION

The aerobrake structural system consists of both the support truss and the hexagonal heatshield panels and the design of each will be treated in separate sections of the paper. The following assumptions however, were used when designing both parts of the structural system:

- Aerobrake diameter = 1440 inches (120 feet).
- Attached spacecraft mass (= total vehicle mass - aerobrake mass) is 450,000 lbm.
- A uniform pressure exists over the entire aerobrake surface.
- The maximum deceleration rate is 6 g's (resulting in a pressure of 2 psi).
- The truss and hexagonal panels are flat.
- Room temperature material properties are used.

Support Truss

The material used in the support truss struts is a high modulus graphite/epoxy system (see reference 11) assumed to have the following unidirectional lamina properties:

- E_1 = 44.3 Msi
- E_2 = 1.0 Msi
- G_{12} = 0.85 Msi
- ν_{12} = 0.3
- ρ = .063 lbm/in^3

where G is the material shear modulus. A factor of safety of 1.4 was assumed for truss design, and the truss applied loading was multiplied by this value when obtaining the strut internal loads used for strut sizing. Compression strength limits for laminated composites are reported in reference 12 and led to 100 ksi being chosen as the the maximum allowable stress for the struts. In addition, the minimum gauge strut thickness was assumed to be 0.06 inches (12 plies at .005 inch thickness). In order to estimate the total truss mass (which consists of the total strut mass plus the total joint mass), the total joint mass was assumed to be equal to the total strut mass.

Selecting the layup angle for the support truss struts was the first issue to be addressed. The buckling stress, σ_{LB}, and strain for a thin walled cylinder are calculated using equations in reference (9), and are shown as a function of the wall layup angle in figure 6. For low (0° - 10°) and high (80° - 90°) values of theta, the buckling modes contain both axial and circumferential waves. For all other values of theta, where the buckling stress is nearly constant, the buckling mode shapes are axisymmetric. The buckling stress, σ_{LB}, for each layup angle (see figure 6), together with the associated effective modulus, E_{eff}, and the strut geometry, were substituted into equation (9) to calculate the value of C_1 for each layup angle.

Minimum mass strut designs, calculated for strut layup angles from 0° to 15° using equations (13) - (15), are shown in figure 7. As the layup angle is increased from 0°, the local buckling stress increases as shown in figure 6. At the same time however, E_{eff}, which is critical for Euler buckling stress, is rapidly decreasing. For a given length strut, the minimum mass design occurs at a ±10° layup angle, where the local and Euler buckling stresses are equal. The calculated value of C_1 for $\theta = 10°$, is .0867. The load ranges where minimum mass, minimum gauge, and maximum allowable stress conditions apply are shown for a strut with ± 10° layup in figure 8. The minimum gauge lines correspond to a 120 foot diameter aerobrake with 8, 6, 4, and 2 rings. The knockdown factors assumed for this strut design are 0.7 for local buckling, and 0.9 for Euler buckling.

When the uniform pressure load is applied to the support truss, the maximum compressive strut loads occur in the core struts which connect to the nodes at the truss load points (these are the reaction points for the static truss analysis). The variation in actual (as opposed to design) maximum strut axial compressive load as the number of truss load points are increased is shown for 3 different g levels in figure 9. The strut design load is obtained by multiplying the results in figure 9 by 1.4 (the factor of safety). The number of truss load points used, represents how the spacecraft (modules, tanks, landers, etc.) is attached to the back of the aerobrake support truss. These results show that the magnitude of load in the most heavily loaded truss strut decreases significantly as the spacecraft systems are distributed over more of the support truss back surface (thus increasing the number of load points).

The strut diameter associated with the maximum loads in figure 9 are shown in figure 10 for a 2, 4, 6, and 8 ring truss as the aerobrake deceleration is varied from 2 to 6 g's. The design load was used to size the struts (= 1.4 x the values in figure 9) and 6 truss load points were assumed for all trusses. The results show that the maximum strut diameter is not very sensitive to deceleration. Since decreasing the number of rings results in longer struts, the maximum strut diameter must increase to satisfy the Euler buckling criteria. Figure 11 shows that the maximum strut diameter is also relatively insensitive to the number of truss load points for 2, 4, and 6 g's deceleration. The relative insensitivity of strut diameter to load can be explained by noting in equation (14), that the strut radius increases by only the 1/3 power of the applied load.

Although only the maximum truss strut loads have been discussed previously, the total support truss has struts with a wide range of applied loadings. For example, figure 12 shows how the number of truss struts are distributed according to their applied loadings for load ranges of 10,000 lbf. These results are for a 6 ring truss (954 total struts), at 2 g's deceleration and with either 3 or 6 truss load points. The majority of the total truss struts are very lightly loaded (in the 0 - 10,000 and 10,001 - 20,000 lbf ranges) while only a few are in the most heavily loaded range (80,001 - 90,000 lbf for six truss load points, and 160,001 - 170,000 lbf for 3 truss load points).

An efficient design, which minimizes the support truss mass, must clearly take advantage of the strut load distribution shown in figure 12. For example, if only one truss strut design is used throughout the truss, that strut design must be capable of carrying the maximum load existing in the truss. This design would be inefficient because it would result in a large number of struts operating at very low stress levels.

A truss design procedure which makes use of truss strut load distribution information (as given in figure 12 for example) proceeds as follows: The number of different strut designs allowed (where the struts are designed for specific load carrying ranges) is specified. Strut designs and masses are then calculated for 10,000 lbf increments in load (ie. a strut is designed which can carry 10,000 lbf, 20,000 lbf, 30,000 lbf etc. up to the maximum strut load existing in the truss). Design loads are then chosen (always designing one strut for the maximum load) and the number of struts which fall into the range for each design load are multiplied by the associated strut mass, and the masses summed for all strut designs to obtain the total strut mass. The total strut mass will change as different values of design load are chosen, and masses are calculated for all possible combinations to determine which will give the minimum total strut mass. For example, using the truss strut load distribution with three load points given in figure 12, the minimum mass support truss using 3 different strut designs results in; 633 struts with loads ranging from 0 - 20,000 lbf receiving the 20,000 lbf strut design, 249 struts with loads ranging from 20,001 - 50,000 lbf receiving the 50,000 lbf strut design, and 72 struts with loads ranging from 50,001 - 170,000 lbf receiving the 170,00 lbf strut design.

The total strut mass reduction possible when using more than one strut design is shown in figure 13. Total strut mass is given for a 6 ring truss with 2 g's deceleration loading and for several different number of truss load points. The 1 strut design must use a strut sized to carry the maximum load in all locations throughout the truss. Using two different strut designs reduces the truss mass by a factor of two, while using three different strut designs results in slightly larger mass reductions. The N design case assumes a different strut design for each 10,000 lbf load range and serves as a practical limit on the minimum truss mass obtainable using this design procedure. Very little mass reduction is obtained by using more than 3 strut designs, so 3 designs was selected for all subsequent truss studies. Figure 13 shows that this design procedure also results in a truss which has a total mass which is relatively insensitive to the number of load points. This happens because the mass of the heavily loaded struts no longer dominate the total truss mass.

The number of struts with a given axial stress (for ranges of 10 ksi) are shown for the cases of 1 strut design and 3 strut designs in figure 14. A 6 ring truss with 2 g's deceleration loading and three load points was used to obtain these results. The mass reductions possible using 3 different strut designs can be achieved while maintaining acceptable stresses ($\leq$ 100 ksi axial) throughout the truss. The out-of-plane displacements for the support truss described in figure 14, are shown for the 1 and 3 strut designs in figure 15. Although the maximum displacement for the 3 strut design (4.91 inches) is approximately 80 percent greater than the maximum displacement for the 1 strut design (2.70 inches), both displacements are very small when compared to the aerobrake diameter. The maximum displacement can be reduced by distributing the spacecraft components more evenly over the aerobrake truss surface, resulting in more truss load points. The strut axial stress distribution associated with the truss configuration referenced in both figures 14 and 15 is shown for the truss top surface in figure 16. The maximum stress, occurring in the core struts connected to the load points, are less than the 100 ksi allowable. The maximum stresses in the surface struts are less than 50 percent of the truss maximum.

The variation of total strut mass with increasing deceleration rate for a 6 ring truss with 6 truss load points is shown in figure 17. Once again, large mass reductions are possible when the 3 strut design is used instead of the 1 strut design. In addition, the total strut mass for the 3 strut design is less sensitive to increasing deceleration. For example, tripling the deceleration rate (and thus the applied pressure on the aerobrake) results in only a 63 percent increase in total strut mass for the 3 strut design.

Figure 18 shows the change in total strut mass as the number of truss rings are varied for a truss supported at 6 load points, decelerating at 2 g's, and having 3 strut designs. Since the total strut mass of a 8 ring truss is only 36 percent greater than the total mass of a two ring truss, the number of rings in the truss does not have a large influence on the truss mass.

Hexagonal Heatshield Panels

The hexagonal heatshield panels have a sandwich construction, with graphite epoxy face sheets and an aluminum honeycomb core. The face sheets are assumed to have a quasi-isotropic layup, resulting in an effective modulus, E_f, of 14.4×10^6 psi. In addition, the assumed material density is .063 lbm/in^3 and the minimum gauge face sheet thickness is .04 inches. The aluminum honeycomb core selected has a density of .00231 lbm/in^3 (4.0 lbm/ft^3). For a hexagonal panel simply supported at three of its verticies (see figure 3), the value of α is .00777 (see equation 17). Finally, two different thermal protection system designs were considered for the heatshield (which must be attached to the panel surface). The areal densities of the two designs are .0142 lbm/in^2 and .0069 lbm/in^2. The thermal protection system mass was assumed not to vary with deceleration rate in this study.

The face sheet thickness for a minimum mass panel design (see equation (23)) varies with the panel stiffness parameter as shown in figure 19. For panel stiffness parameters less than approximately 8.0×10^8, the minimum gauge face sheet thickness of .04 inches must be used. The core thickness for a minimum mass panel, as a function of the panel stiffness parameter, is shown in figure 20. Values of core thickness which correspond to the face sheet thickness being held constant at its minimum gauge value are also shown in the figure. For panel stiffness parameters less than approximately 8.0×10^8, these values of the core thickness must be used along with the minimum gauge face sheet thickness. For a representative aerobrake design having 8 rings, decelerating at 4 g's, and having a panel deflection limit of $(w_{max}/a) = .001$, the panel stiffness parameter is approximately 1.5×10^9. The associated face sheet and core thicknesses are .049 and 5.4 inches respectively (see figures 19 and 20).

The aerobrake hexagonal panel structural mass, which includes the core and face sheets but not the thermal protection system, is shown as a function of the panel stiffness parameter in figure 21. If the panel stiffness parameter is less than 8.0×10^8, the panel mass will be greater than minimum mass because the minimum gauge face sheet thickness constraint is invoked. For example, when the panel stiffness parameter is 1.0×10^8, a panel with minimum gauge facesheets has a mass which is 13.6 percent greater than that of a minimum mass panel. If packaging volume is

critical, constraints might be placed on the maximum heatshield thickness that is allowed. When compared to the minimum mass design, limiting the core thickness to 8 inches for, example, can result in large increases in panel mass for large values of the stiffness parameter (see figure 21).

The hexagonal panel out-of-plane displacement due to a uniform applied pressure loading is shown in figure 22. The panel in this example has a stiffness parameter of 1.5×10^9 in-lbf, resulting in a core thickness of 5.409 inches and a face sheet thickness of .049 inches (see figures 19 and 20 also). The maximum deflection is approximately .10 inches, and occurs at the panel center. The deflection limit placed on the panel leads to low stresses in the hexagonal panel face sheet (maximum effective stress is only 5.2 ksi).

Total System

Results will now be discussed for the total aerobrake system, which includes the support truss (struts and joints) and the heatshield panels (hex panels and thermal protection system). The mass for a 120 foot diameter aerobrake is given in figure 23. Six truss load points, 2 g's deceleration and 3 different strut designs are assumed in these results. Although the truss mass increases slightly with an increasing number of rings, the truss represents a small fraction of the total aerobrake mass. Large decreases in hexagonal panel mass are possible by increasing the number of rings in the support truss because the panels then have to span a smaller distance, thus reducing the effect of the panel deflection requirement. Total aerobrake masses which are less than or equal to 15 percent of the total spacecraft payload mass (450,000 lbm) are possible for designs with 4 or more rings. The effect of increasing deceleration rate on total aerobrake mass is shown for a 6 ring design in figure 24. Tripling the deceleration rate results in only a 32 to 39 percent (depending on TPS mass) increase in total aerobrake mass.

The packaging volume for a 120 foot diameter aerobrake, which corresponds to the designs discussed in figure 24, is shown in figure 25. The large decrease in hex panel volume with increasing number of rings is a direct consequence of the panel thickness decreasing as its span becomes shorter. The packaging volume required for a 120 foot diameter aerobrake with 6 or 8 rings is only on the order of one Space Shuttle volume. The aerobrake strut and panel part counts are shown as the number of support truss rings are varied in figure 26. The number of struts and panels which must be assembled increase rapidly as the number of rings are increased.

CONCLUDING REMARKS

An aerobrake structural concept, consisting of two primary components; 1) a lightweight erectable tetrahedral support truss, and 2) sandwich hexagonal heatshield panels which, when attached to the truss, form a continuous impermeable aerobraking surface, has been presented. Design equations and computer models were developed to determine the total mass and volume of the aerobrake, as well as design sensitivities to variations in major design parameters.

The results show that a 120 foot diameter aerobrake is viable using the concept presented in this paper (ie., the aerobrake mass is less than or equal to 15 percent of the payload spacecraft mass). Minimizing the aerobrake mass (by increasing the number of rings in the support truss) however, leads to aerobrakes with the highest part count. The total aerobrake mass and packaging volume are dominated by the heatshield (hexagonal panels and thermal protection system) design. Because the hex panel thickness, and thus mass, is so heavily dominated by the maximum deflection criteria, obtaining the correct maximum heatshield deflection value is critical to establishing an accurate aerobrake design.

Good design practice will use at least 3 different strut designs, resulting in a support truss with a total mass which is relatively insensitive to the number of load points or deceleration rate. As the truss struts become shorter (because the number of rings are increased, or the aerobrake diameter is decreased), the struts are sized more by minimum gauge wall thickness or maximum allowable stress constraints, not minimum mass. Graphite epoxy support truss struts must be designed for both Euler column and local wall buckling. For a purely $\pm \theta$ symmetric layup, the associated minimum mass strut design occurs for $\theta = 10^{o}$. Viable support truss designs result in maximum strut diameters of 2.6 - 5.0 inches (for 2 g's deceleration) to 4.4 - 5.9 inches (for 6 g's deceleration).

APPENDIX

Curvature Effects on Aerobrake Structural Performance

A major assumption made to simplify the derivations of the support truss and hexagonal panel design equations, is that the aerobrake had no curvature. Finite element models, which included curvature of a parabolic shape, were developed for both the tetrahedral support truss and the hexagonal sandwich panel. For the small lift to drag ratios which this concept was applied to ($L/D \leq 0.5$) adding curvature results in a 6 foot maximum deviation at the outer diameter of the aerobrake from a flat reference plane passing through the aerobrake's center (see figure A1).

The procedure used to determine the results shown in figure A1, was to design the support truss struts and hexagonal panels using the equations for zero curvature, then apply curvature to the models and determine what differences occurred in structural performance. In the support truss, the curvature reduces the maximum deflection by 10 percent, but only has a minimal effect on both the maximum strut load and the total truss mass (reduced by 2 percent and 0.6 percent respectively). The longer span panel required to represent the curved surface results in only a 0.8 percent increase in total mass. The maximum deflection in the panel was reduced by approximately 16 percent. If the panel was actually designed for this reduced amount of deflection, the core thickness would be decreased by approximately 5 percent resulting in reduced panel mass. In conclusion, for the values of L/D considered, assuming no curvature for the aerobrake simplifies the equations used for preliminary design, but does not significantly impact the aerobrake total mass and packaging volume.

REFERENCES

1. Pioneering the Space Frontier: The Report of the National Commission on Space. Bantam Books, New York, 1986.

2. Cirillo, William M.; Kaszubowski, Martin J.; Ayers, J. Kirk; Llewellyn, Charles P.; Weidman, Deene J.; and Meredith, Barry D.: Manned Mars Mission Accommodation - Sprint Mission. NASA TM-100598, April 1988.

3. Mikulas, Martin M. Jr.; and Dorsey, John T: An Integrated In-Space Construction Facility for the 21st Century. NASA TM-101515, November 1988.

4. Walberg, Gerald D.: A Review of Aerobraking for Mars Missions. Presented at the 39th Congress of the International Astronautical Federation, October 8 - 15 , 1988, Bangalore, India. Paper No. IAF-88-196.

5. Heard, Walter L.; Watson, Judith J.; Ross, Jerry L.; Spring, Sherwood C.; and Cleave, Mary L.: Results of the ACCESS Space Construction Shuttle Flight Experiment. Presented at the AIAA Space Systems Technology Conference, San Diego, California; June 9 - 12, 1986. AIAA Paper No. 86-1186-CP.

6. Rhodes, Marvin D.; Will, Ralph W.; and Wise, Marion A.: A Telerobotic System for Automated Assembly of Large Space Structures. NASA TM-101518, March 1989.

7. Mikulas, Martin M. Jr.; Bush, Harold G.; and Card, Michael F.: Structural Stiffness, Strength and Dynamic Characteristics of Large Tetrahedral Space Truss Structures. NASA TM X-74001, March 1977.

8. Jones, Robert M.: Mechanics of Composite Materials. McGraw-Hill Book Company, 1975.

9. Jones, Robert M.: Buckling of Circular Cylindrical Shells with Multiple Orthotropic Layers and Eccentric Stiffeners. AIAA Journal, Vol. 6, No. 12, December 1968.

10. Honeycomb Sandwich Design, Brochure 'E'. Hexcel Products Inc., c.1959.

11. Bowles, David E.; and Tenney, Darrel R.: Composite Tubes for the Space Station Truss Structure. Presented at the 18th International SAMPE Technical Conference, Seattle, Washington, October 7-9, 1986.

12. Shuart, Mark J.: Failure of Compression-Loaded Multi-Directional Composite Laminates. Presented at the AIAA/ASME/ASCE/AHS 29th Structures, Structural Dynamics and Materials Conference, Williamsburg, Virginia, April 18-20, 1988. AIAA Paper No. 88-2293.

AEROBRAKE CONCEPT

AEROBRAKE FEATURES

-Tetrahedral support truss
-Hexagonal sandwich panels heatshield

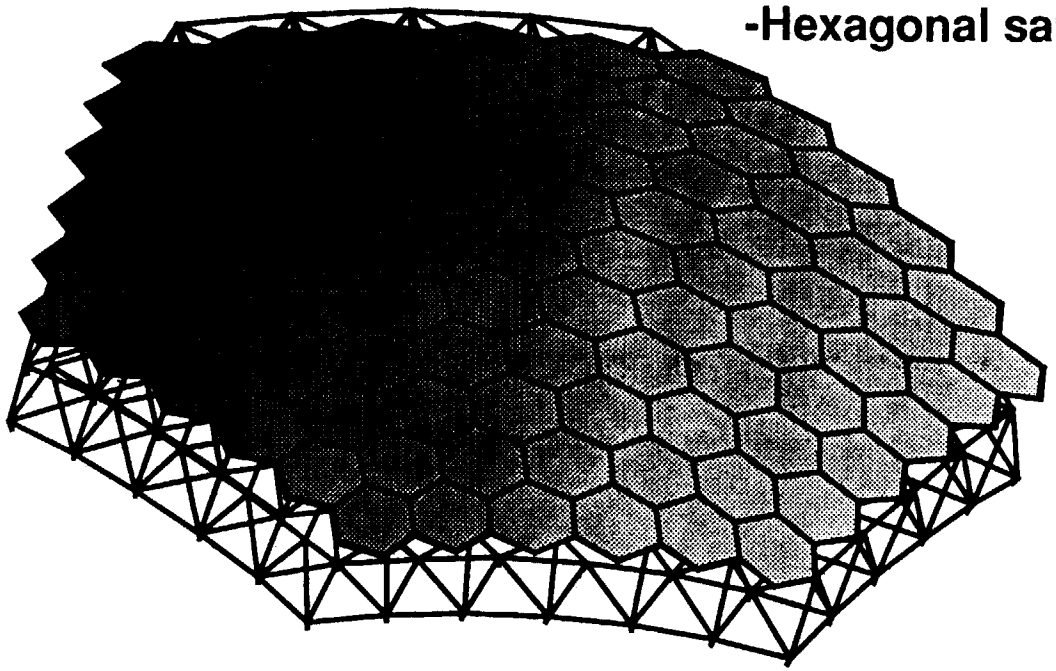

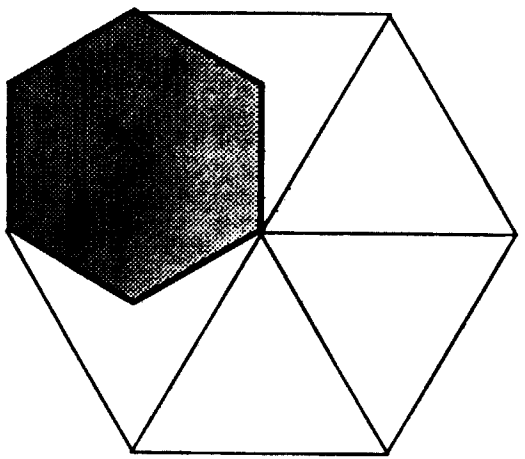

-Heatshield attached
to truss at 3 verticies

NASA

Figure 1.

Dorsey 3/23/89

SUPPORT TRUSS DESCRIPTION

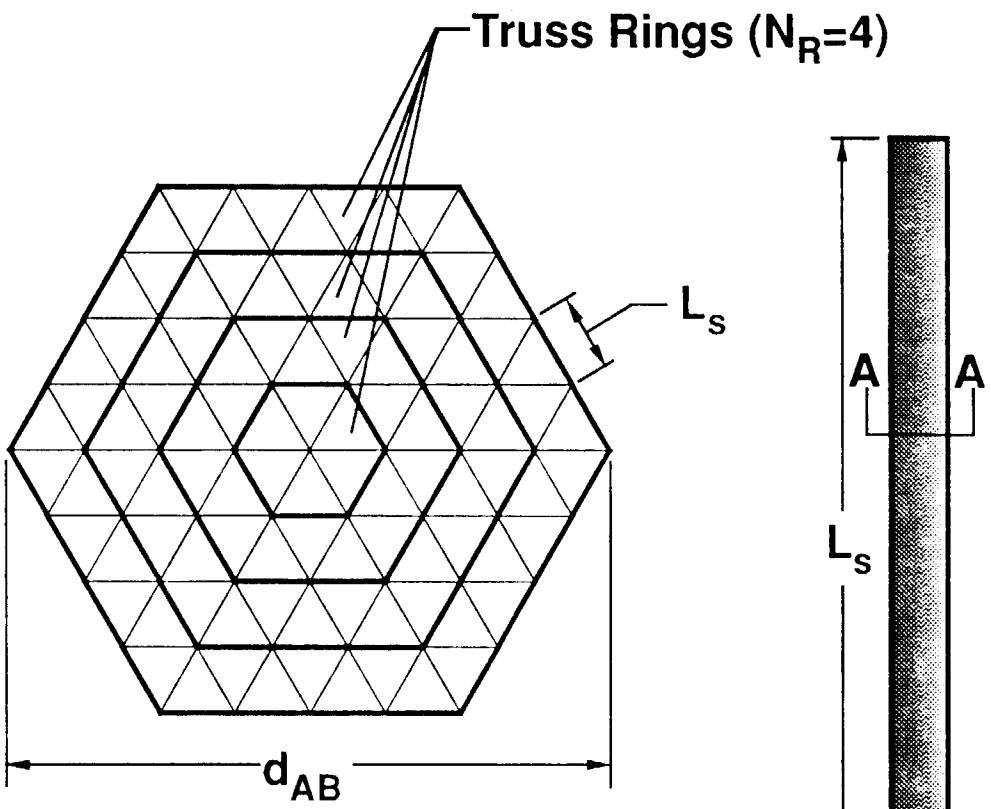

$$L_s = \frac{d_{AB}}{2N_R}$$

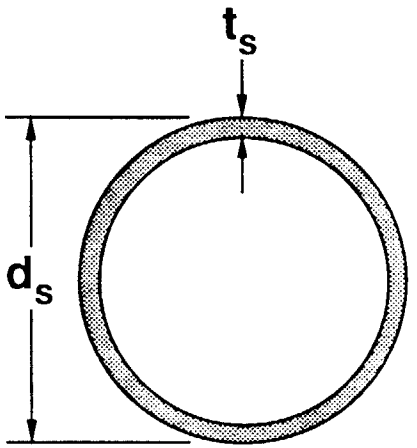

Section A-A

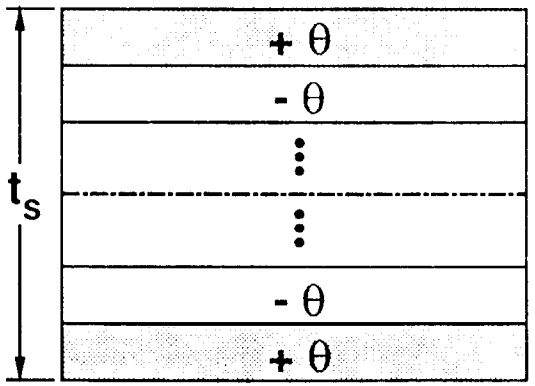

$[+\theta / -\theta]^n_{symmetric}$

NASA

Figure 2.

HEXAGONAL HEATSHIELD PANEL DESCRIPTION

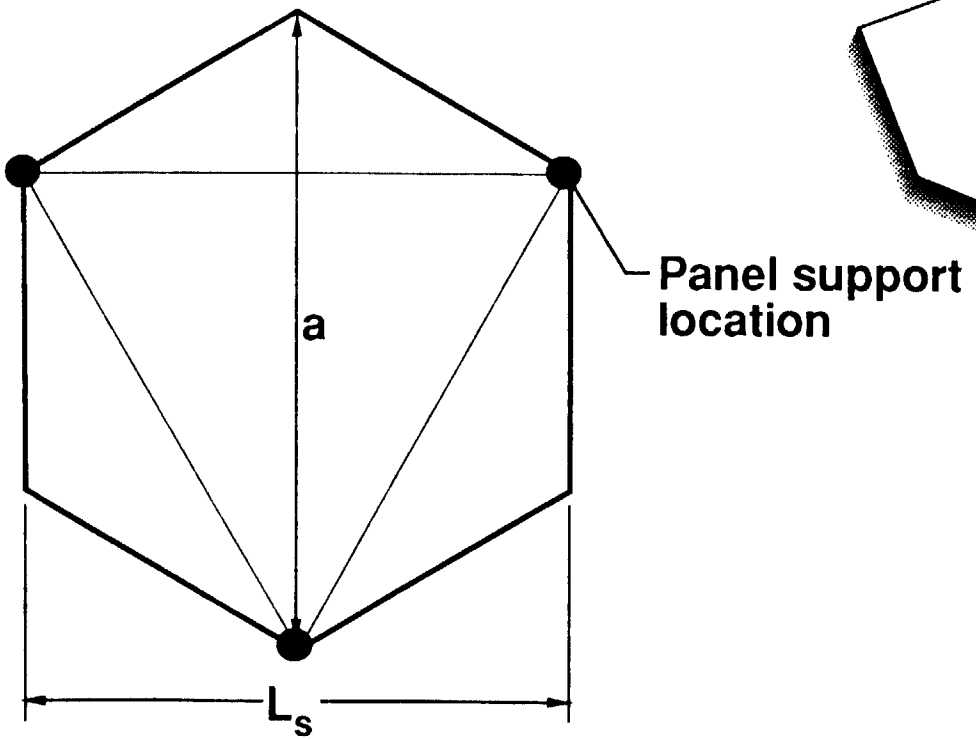

Panel support location

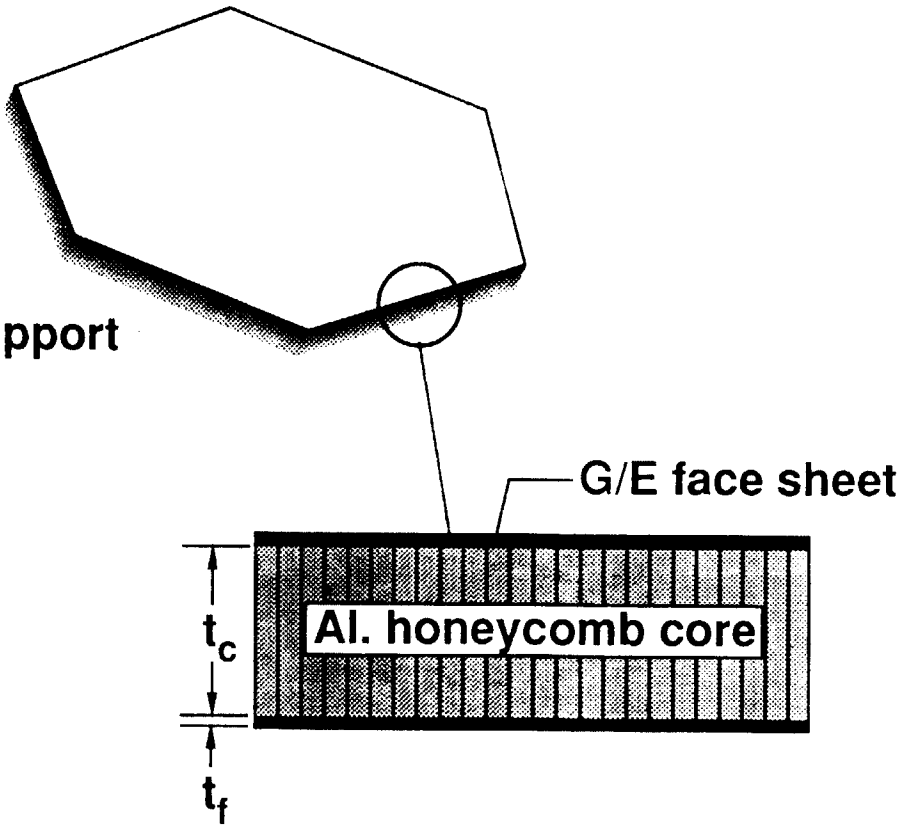

$$a = \frac{2 L_s}{\sqrt{3}}$$

$$D_{HP} = \frac{E_f t_f t_c^2}{2 (1 - \nu_f^2)}$$

Figure 3.

NASA

TWO SEPERATE DESIGN PROBLEMS SOLVED

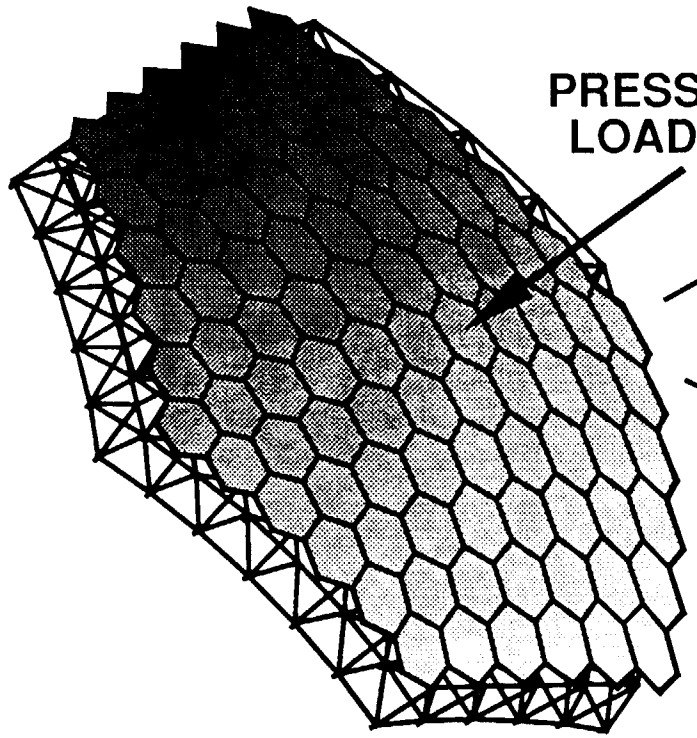

PRESSURE LOADING

Nodal Forces Due to Pressure

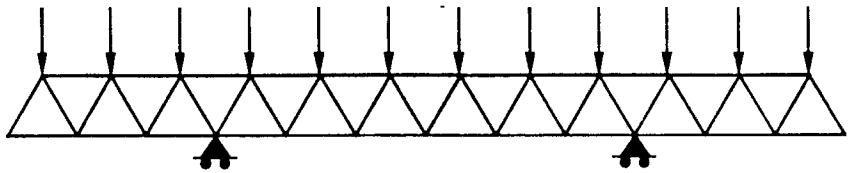

TRUSS

Uniform Pressure Loading

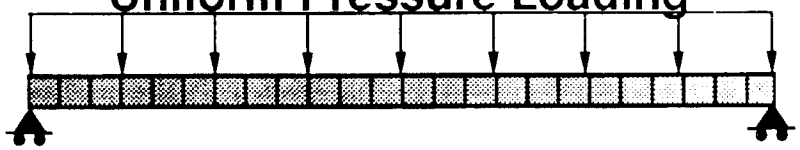

HEATSHIELD

NASA

Figure 4.

Dorsey 4/12/89

AEROBRAKE SUPPORT TRUSS GEOMETRIES CONSIDERED

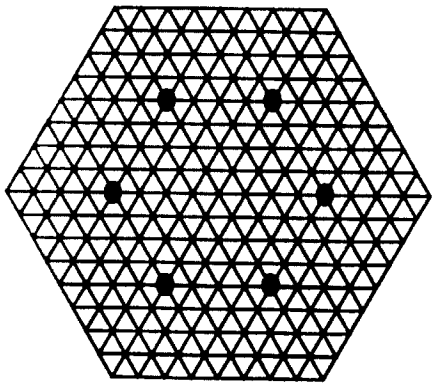

8 RINGS

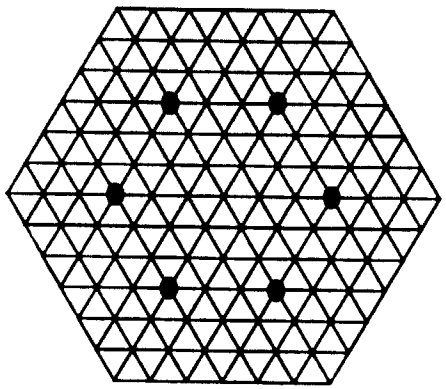

6 RINGS

- TRUSS LOAD POINTS (3, 4, or 6 points)

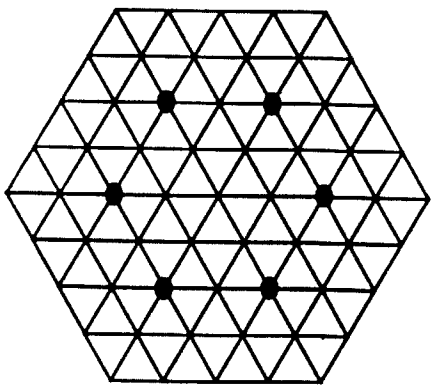

4 RINGS

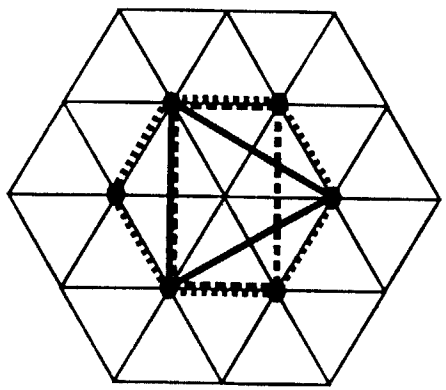

2 RINGS

Figure 5.

TRUSS STRUT LOCAL BUCKLING FOR ± θ LAYUP

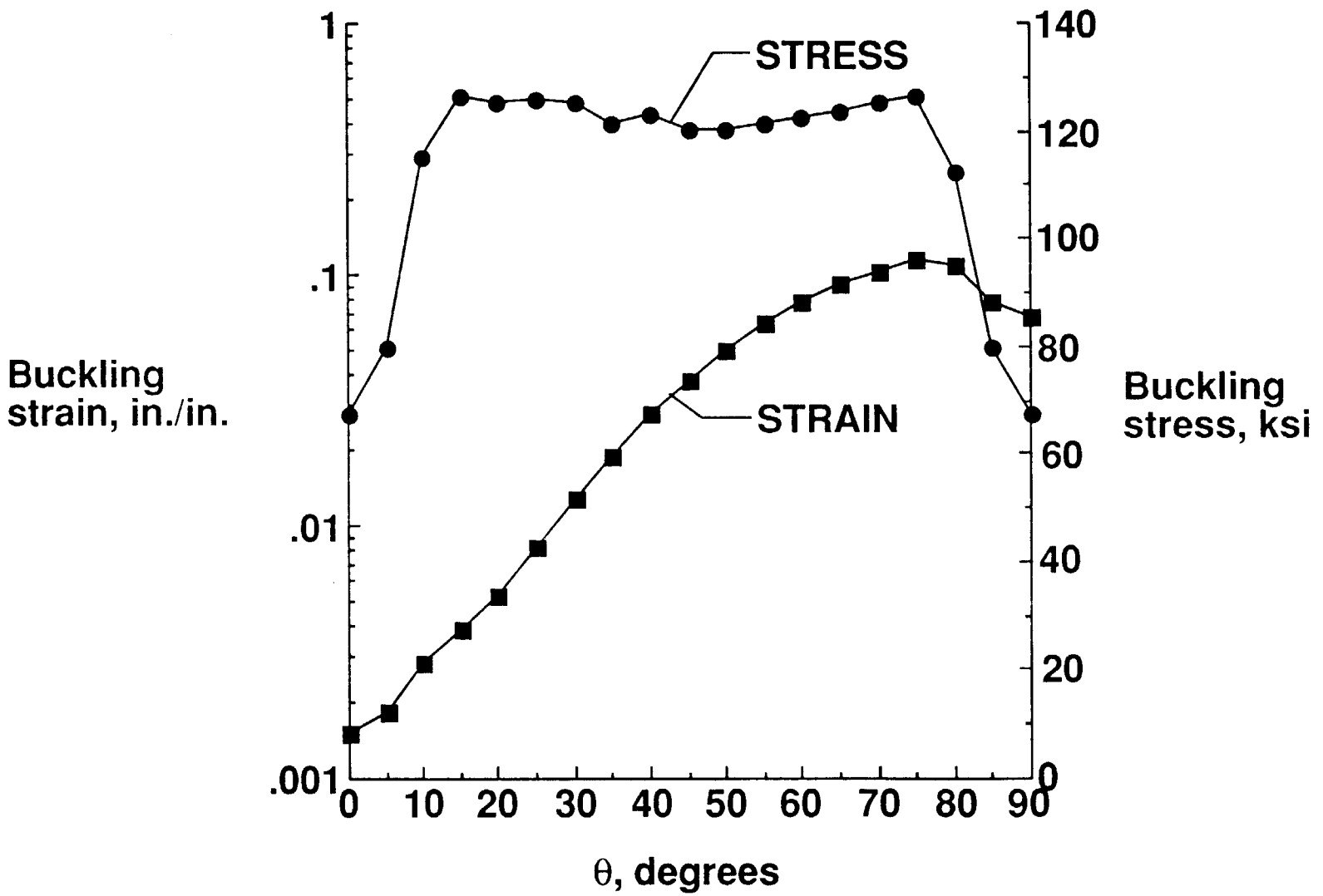

Figure 6.

NASA

Dorsey 6/15/89

± 10° LAYUP RESULTS IN MINIMUM MASS SUPPORT TRUSS STRUT

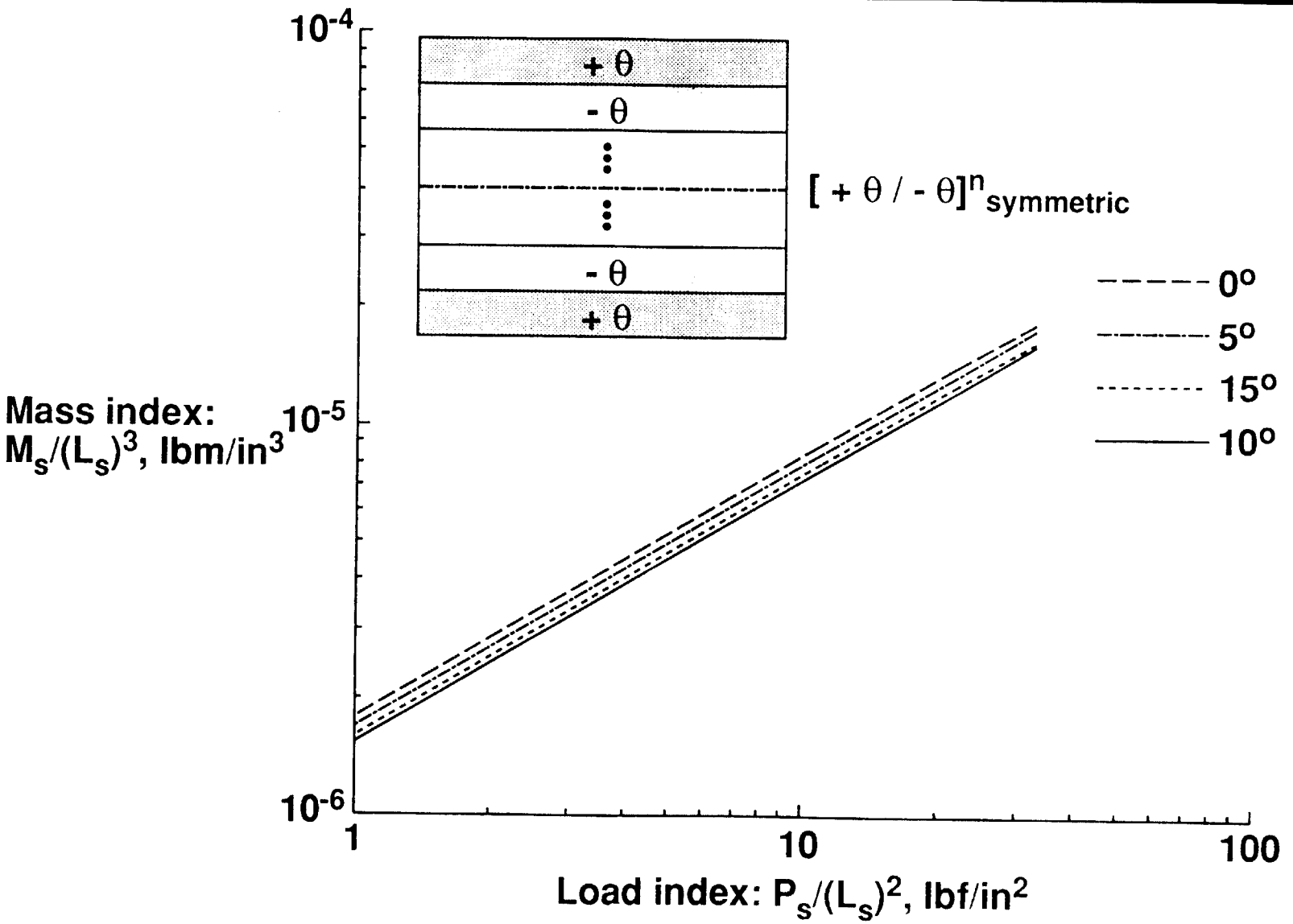

Figure 7.

NASA

Dorsey 6/23/89

SUPPORT TRUSS STRUT MASS VERSUS DESIGN LOAD

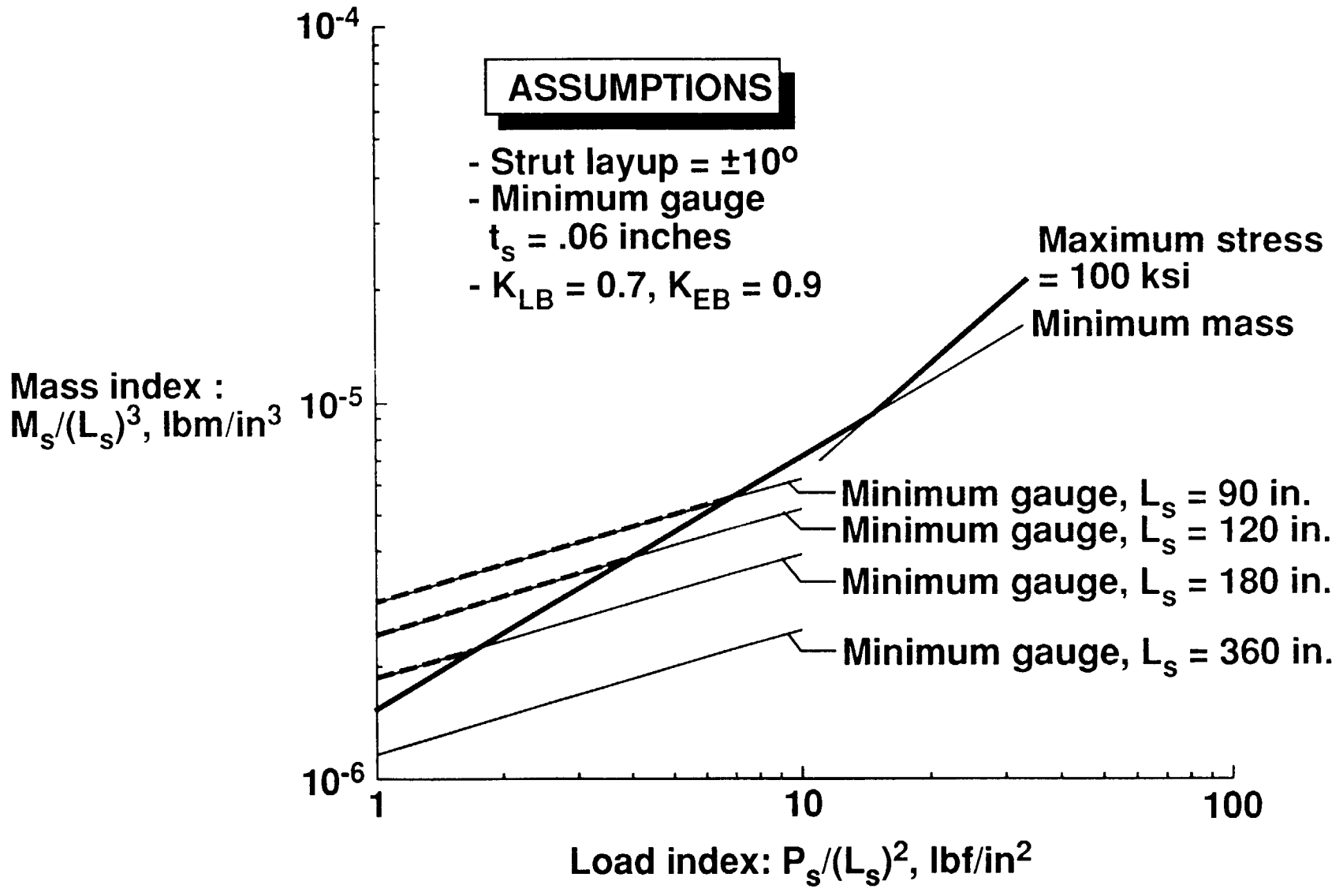

Figure 8.

MAXIMUM STRUT LOAD DECREASES AS THE NUMBER OF SUPPORTS ARE INCREASED

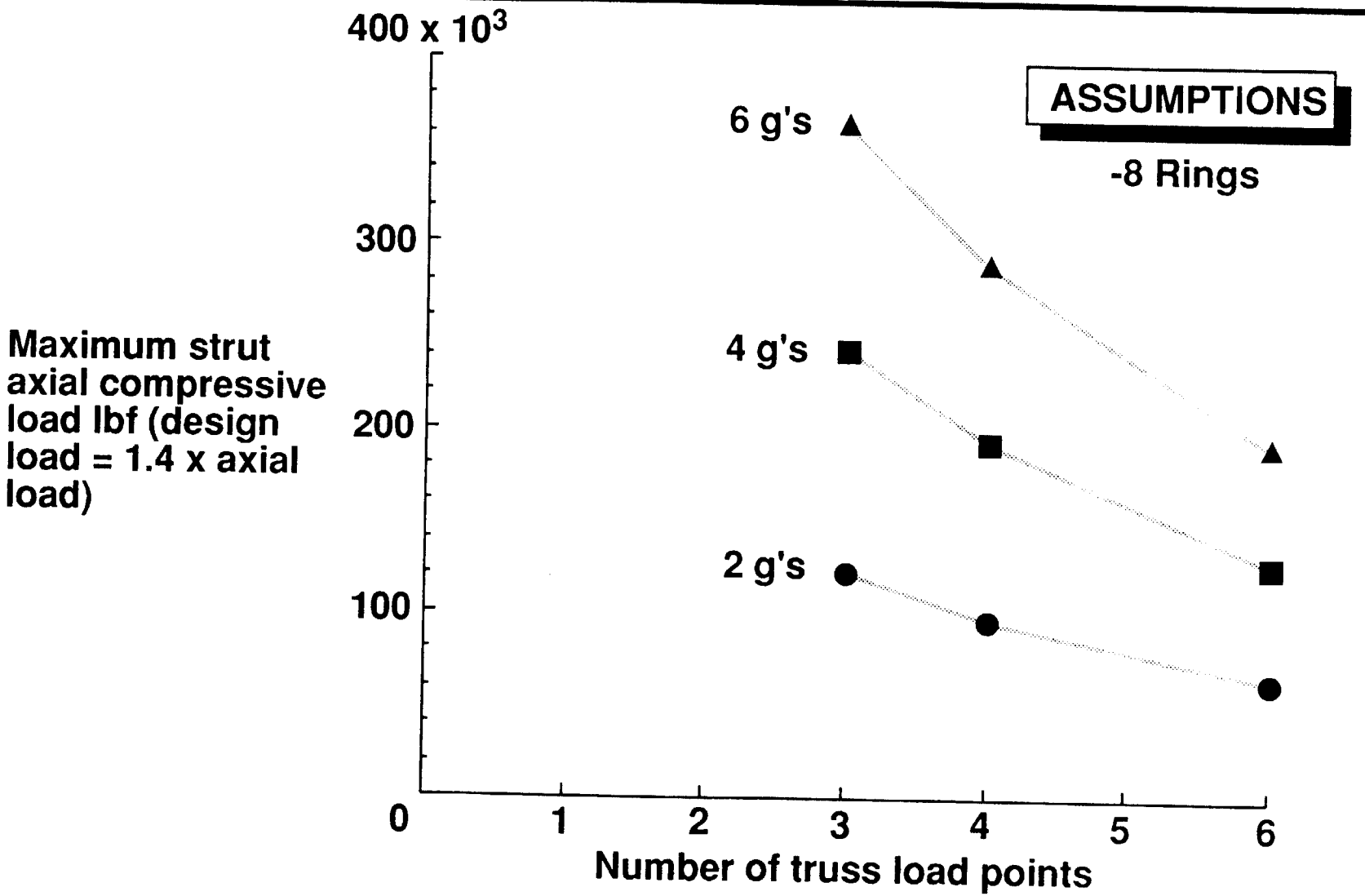

Figure 9.

MAXIMUM TRUSS STRUT DIAMETER INCREASES WITH INCREASING DECELERATION RATE

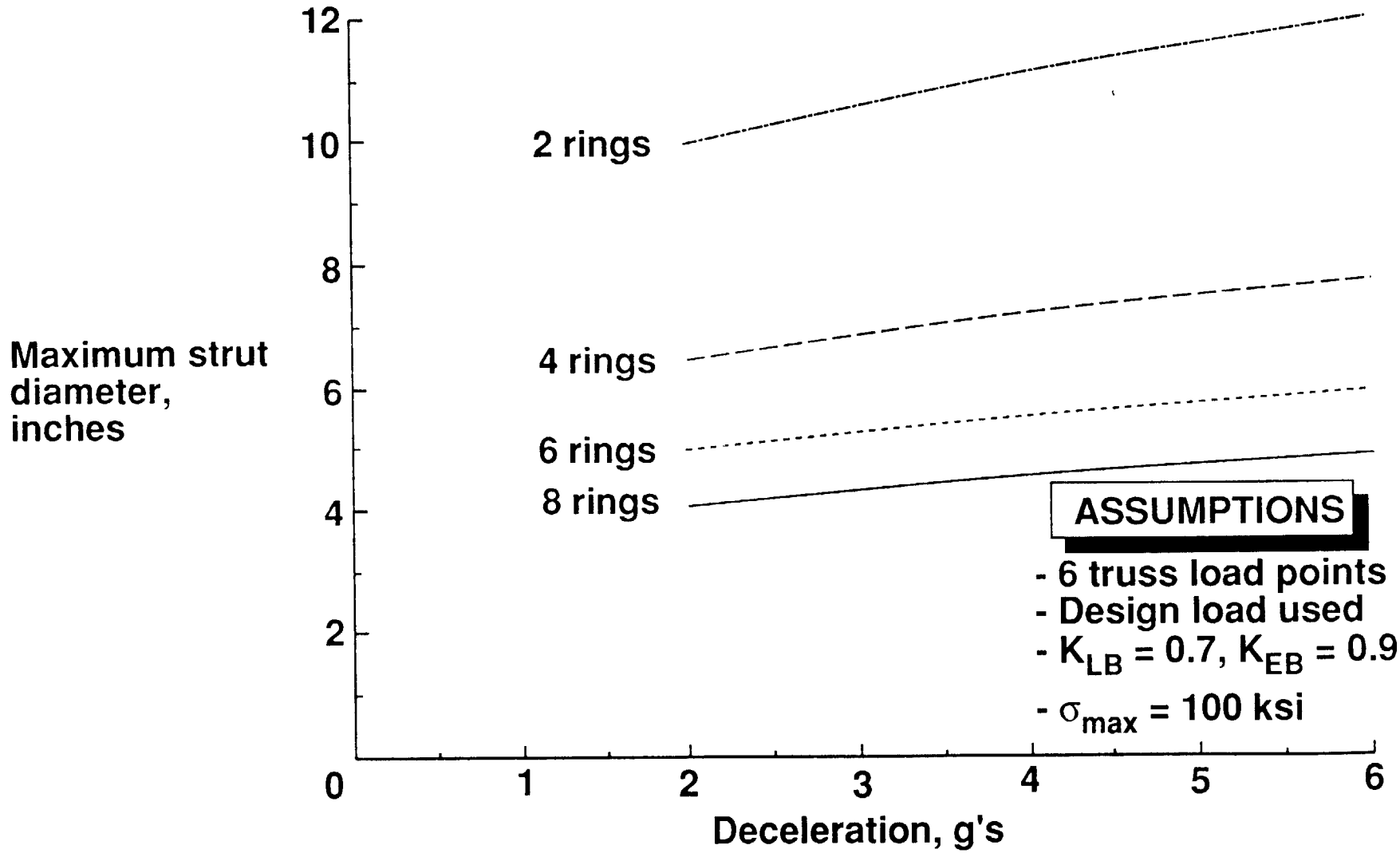

Figure 10.

NASA

Dorsey 7/31/89

MAXIMUM TRUSS STRUT DIAMETER DECREASES WITH INCREASING LOAD POINTS

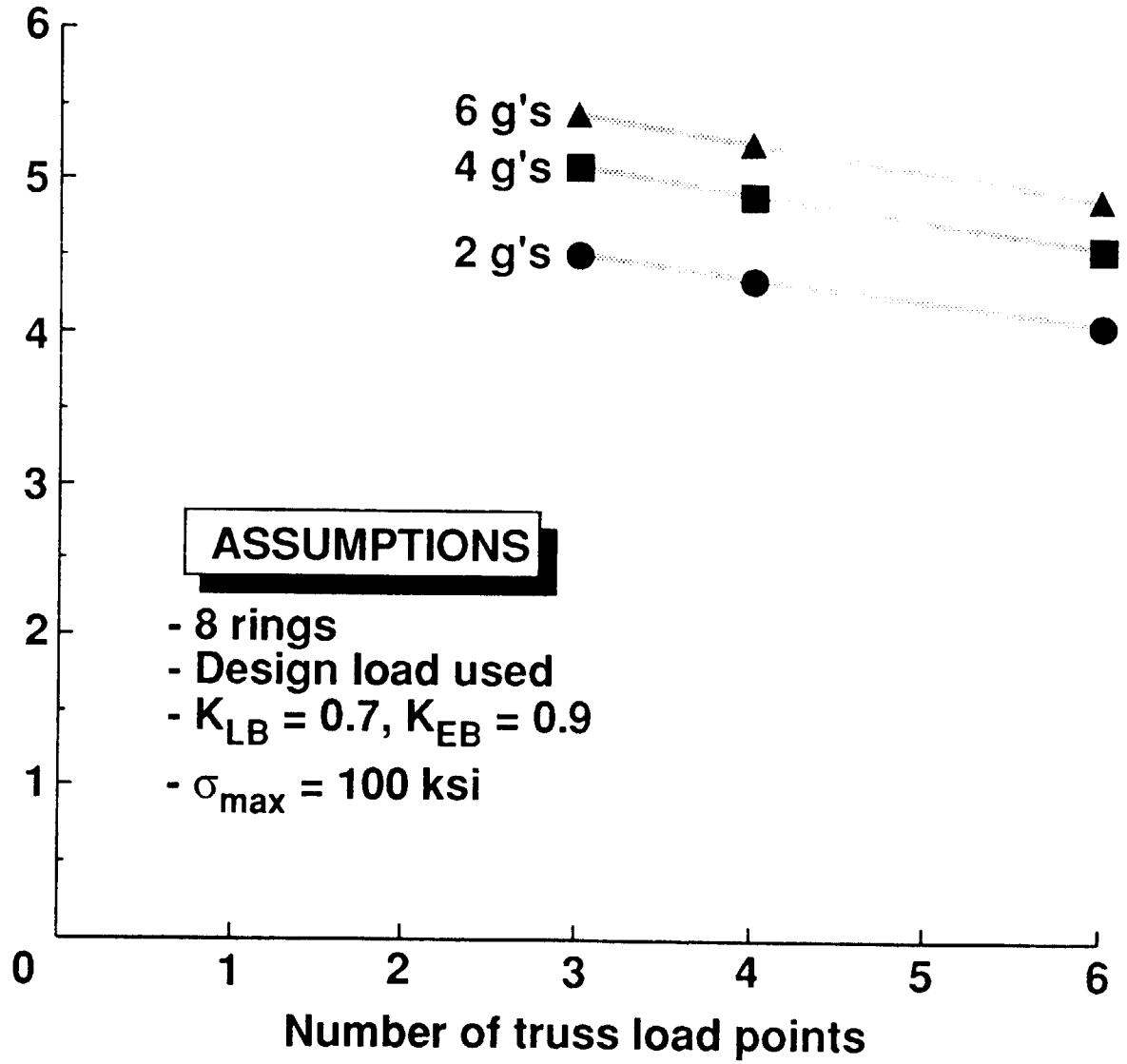

Figure 11.

NASA

Dorsey 7/31/89

TRUSS STRUT LOADS DISTRIBUTION

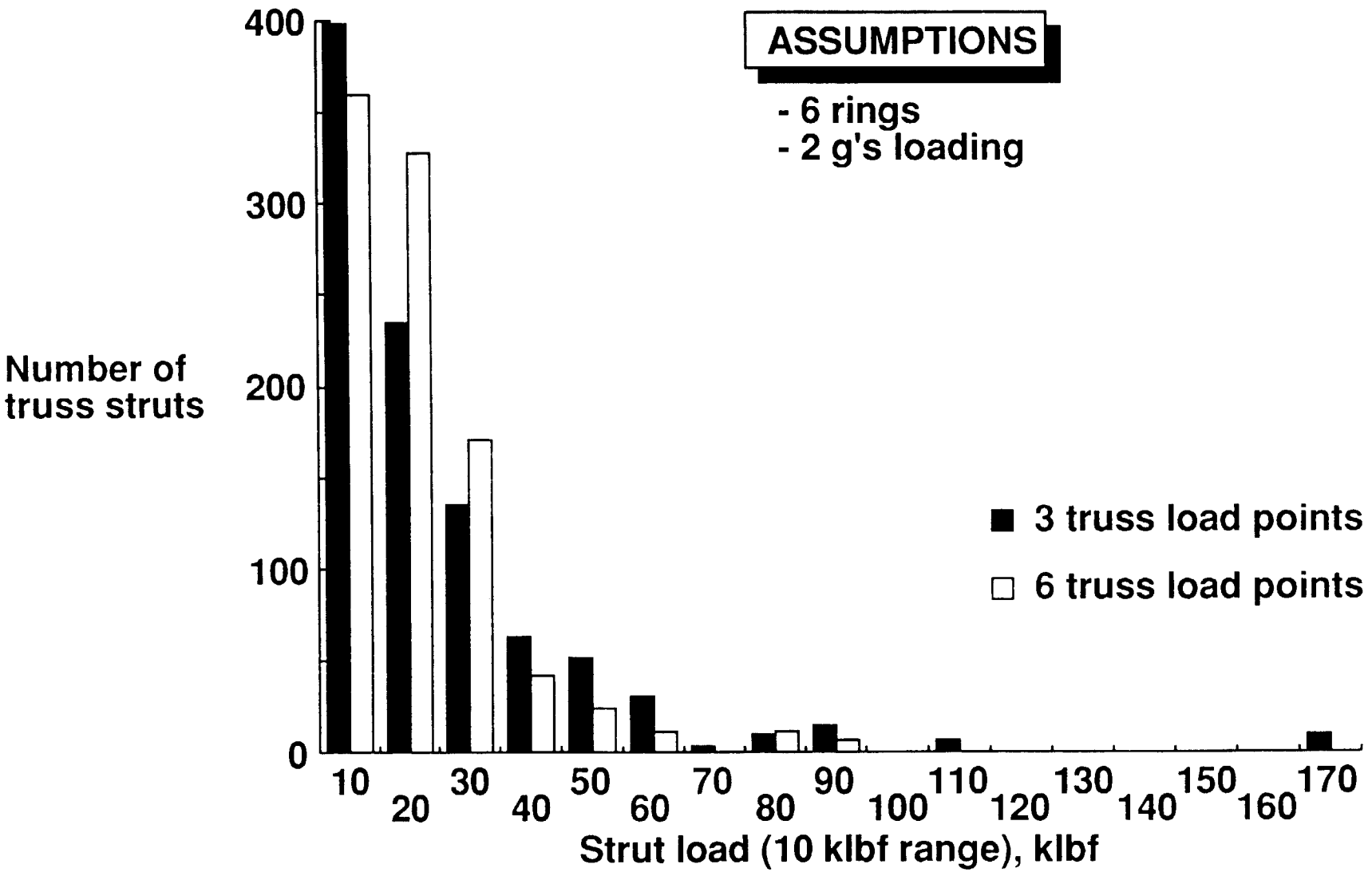

Figure 12.

NASA

Dorsey 5/17/89

USING THREE STRUT DESIGNS RESULTS IN LIGHTWEIGHT TRUSS

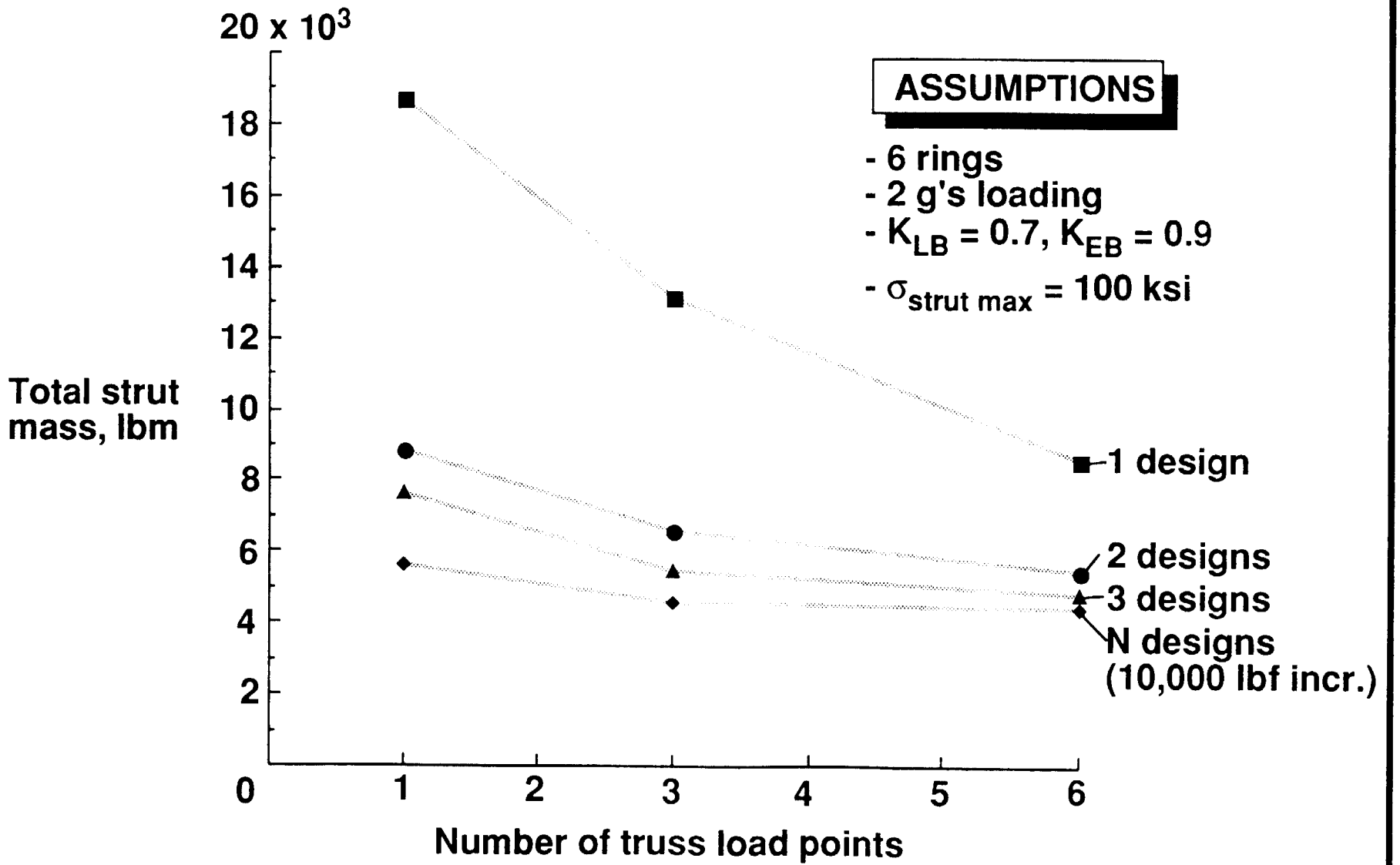

Figure 13.

NASA

Dorsey 8/15/89

TRUSS STRUT STRESS DISTRIBUTION FOR 3 STRUT DESIGN

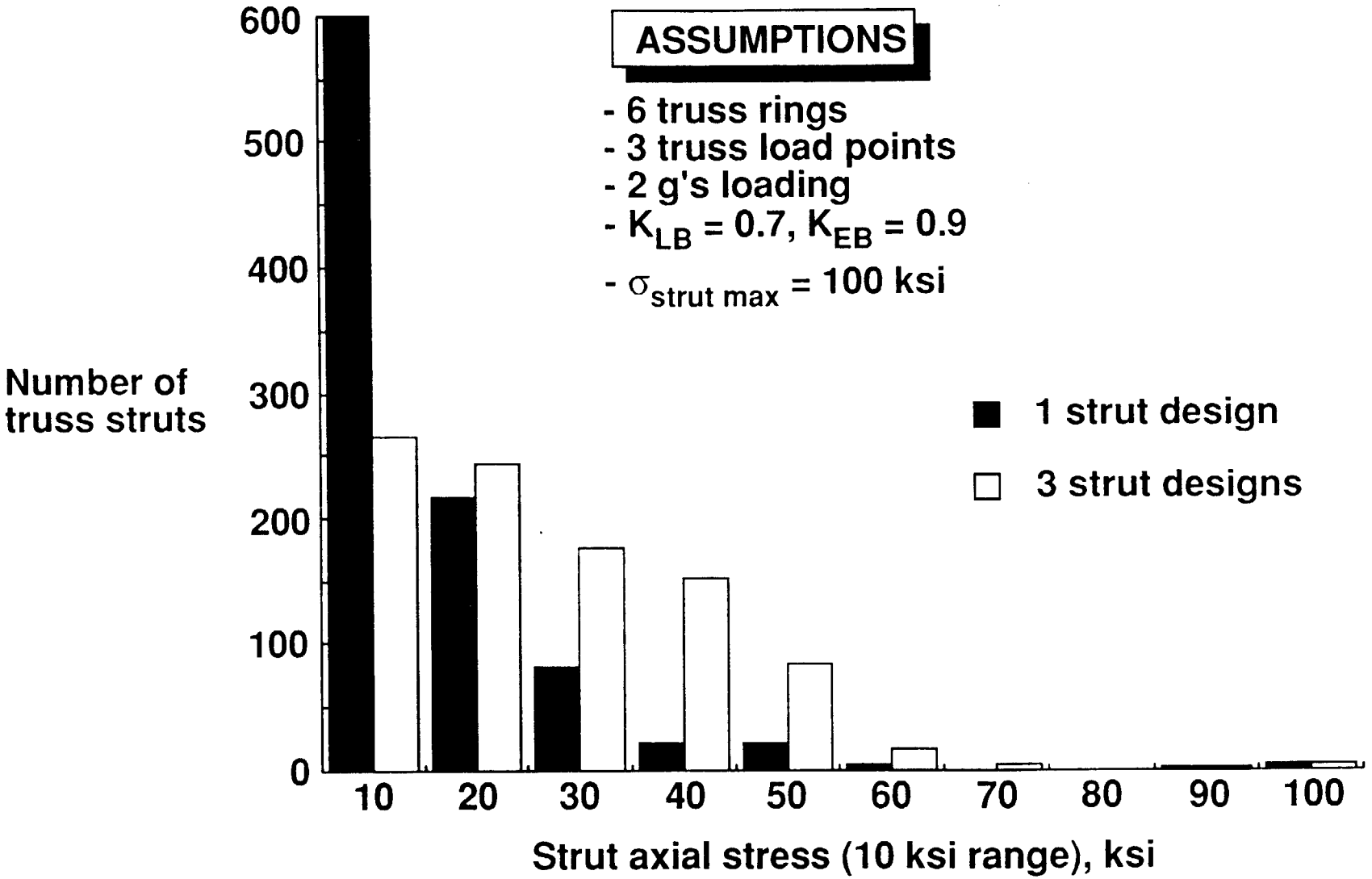

Figure 14.

NASA

Dorsey 7/31/89

SUPPORT TRUSS DISPLACEMENTS DUE TO PRESSURE LOADING

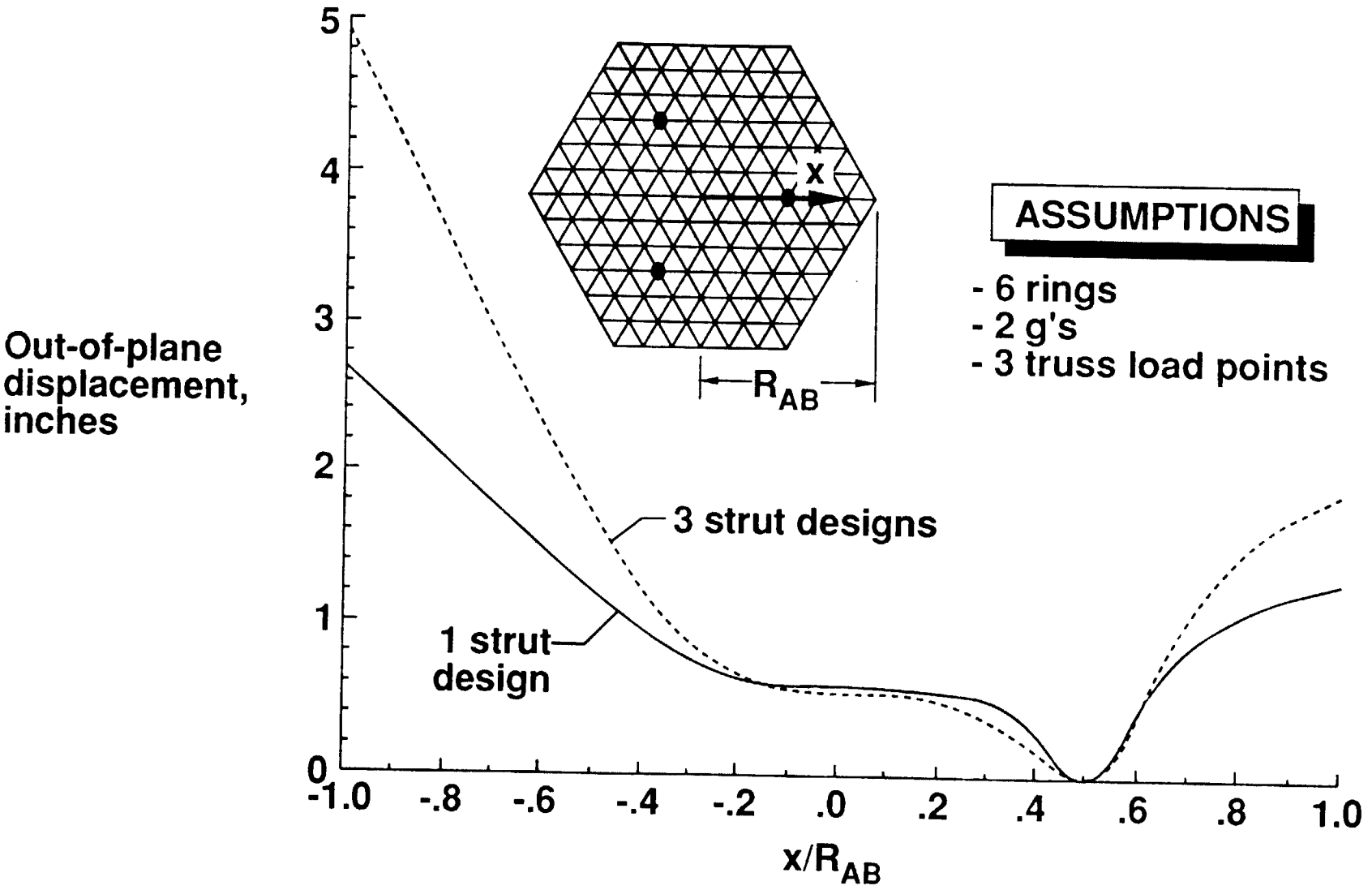

NASA

Figure 15.

Dorsey 7/25/89

SUPPORT TRUSS
STRUT AXIAL STRESS DISTRIBUTION

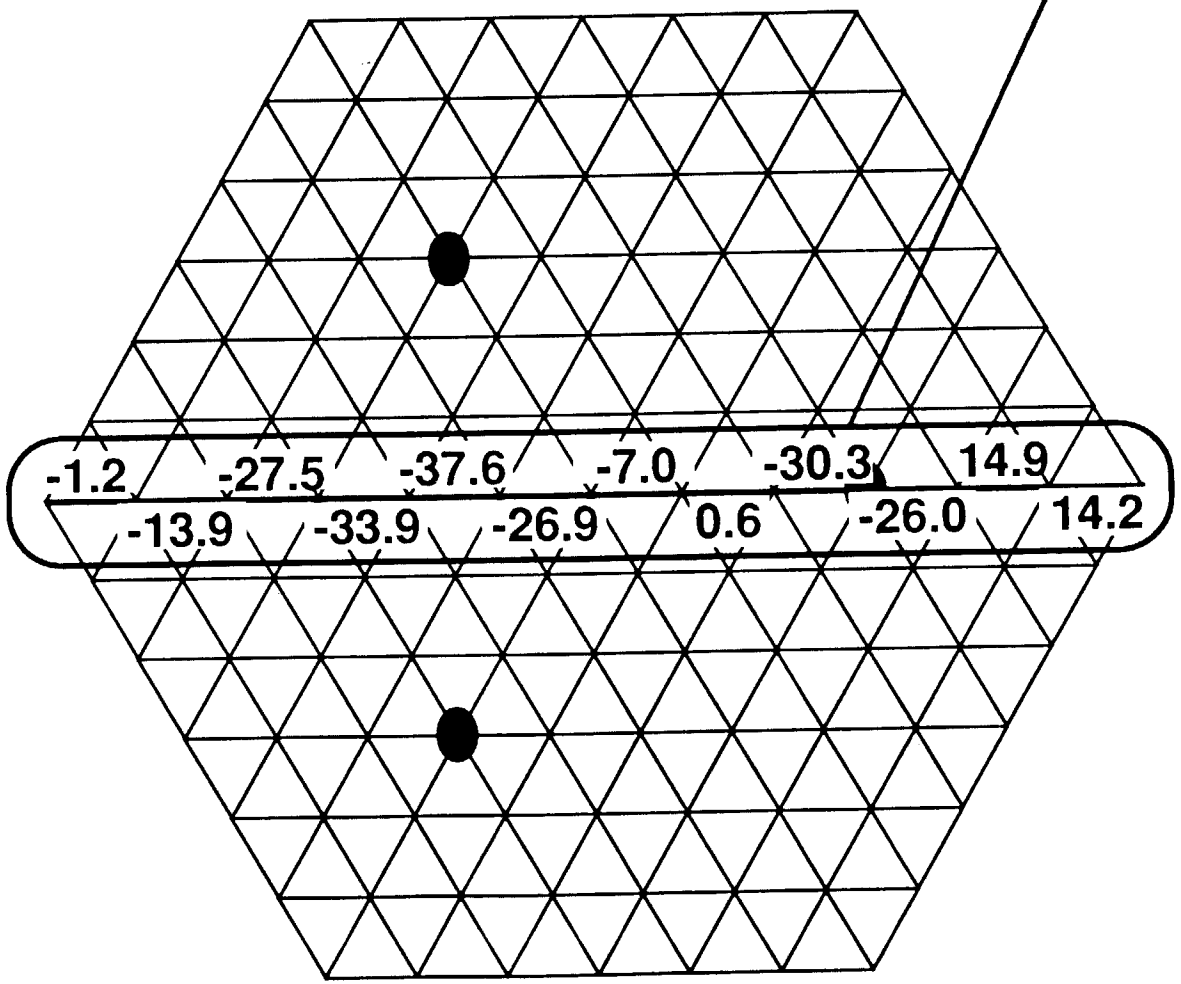

SURFACE STRUT AXIAL STRESS, KSI

MAXIMUM STRUT AXIAL STRESS, KSI

Top surface : - 48.2
Core : - 92.9
Bottom surface : 62.5

ASSUMPTIONS

- 6 rings
- 2 g's
- 3 truss load points
- 3 strut designs
- $\sigma_{strut\ max}$ = 100 ksi
- K_{LB} = 0.7, K_{EB} = 0.9

Figure 16.

NASA

Dorsey 7/31/89

TOTAL STRUT MASS VERSUS AEROBRAKE DECELERATION

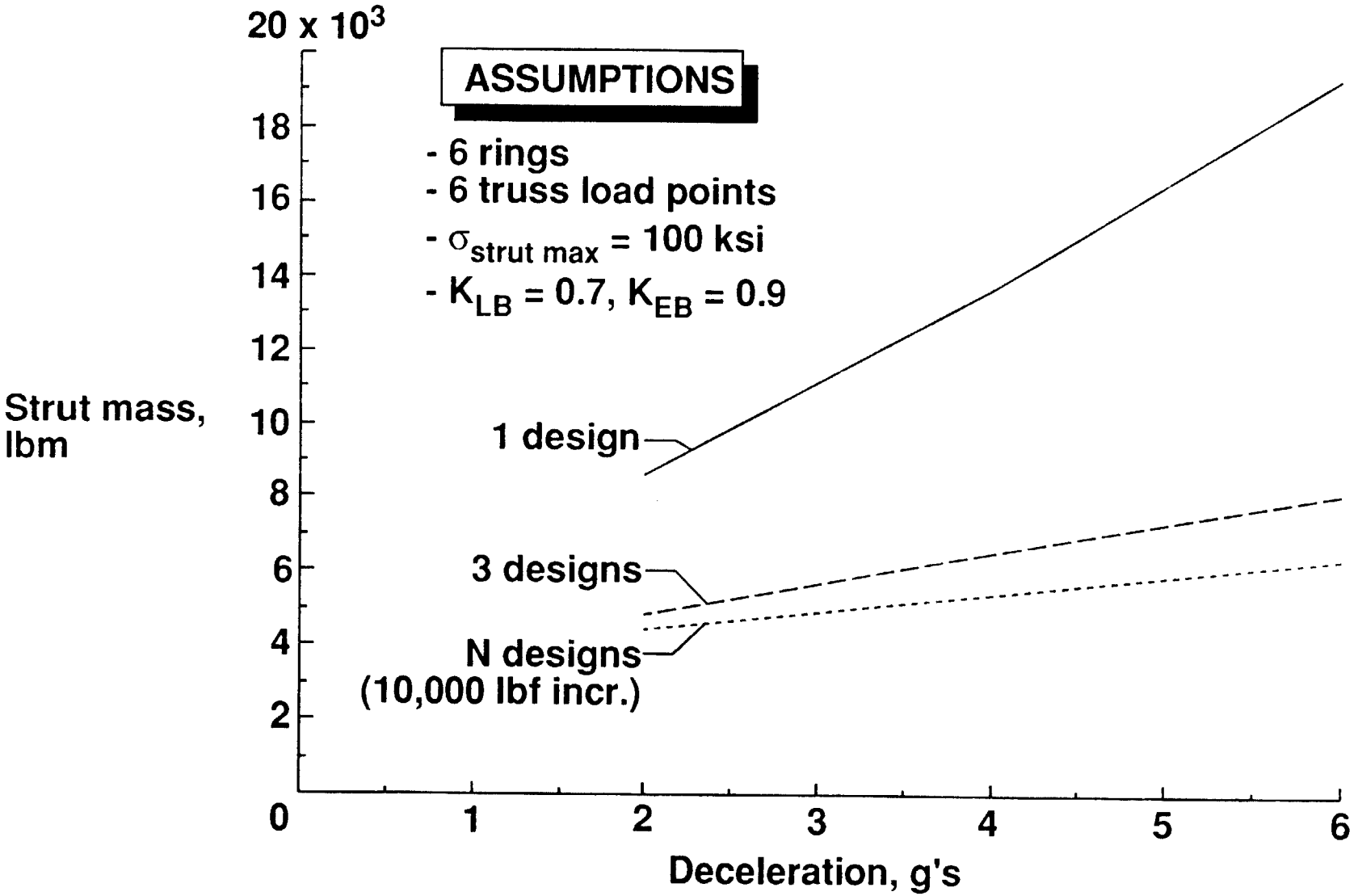

Figure 17.

NASA

Dorsey 7/31/89

INCREASING NUMBER OF TRUSS RINGS RESULTS IN GREATER TRUSS MASS

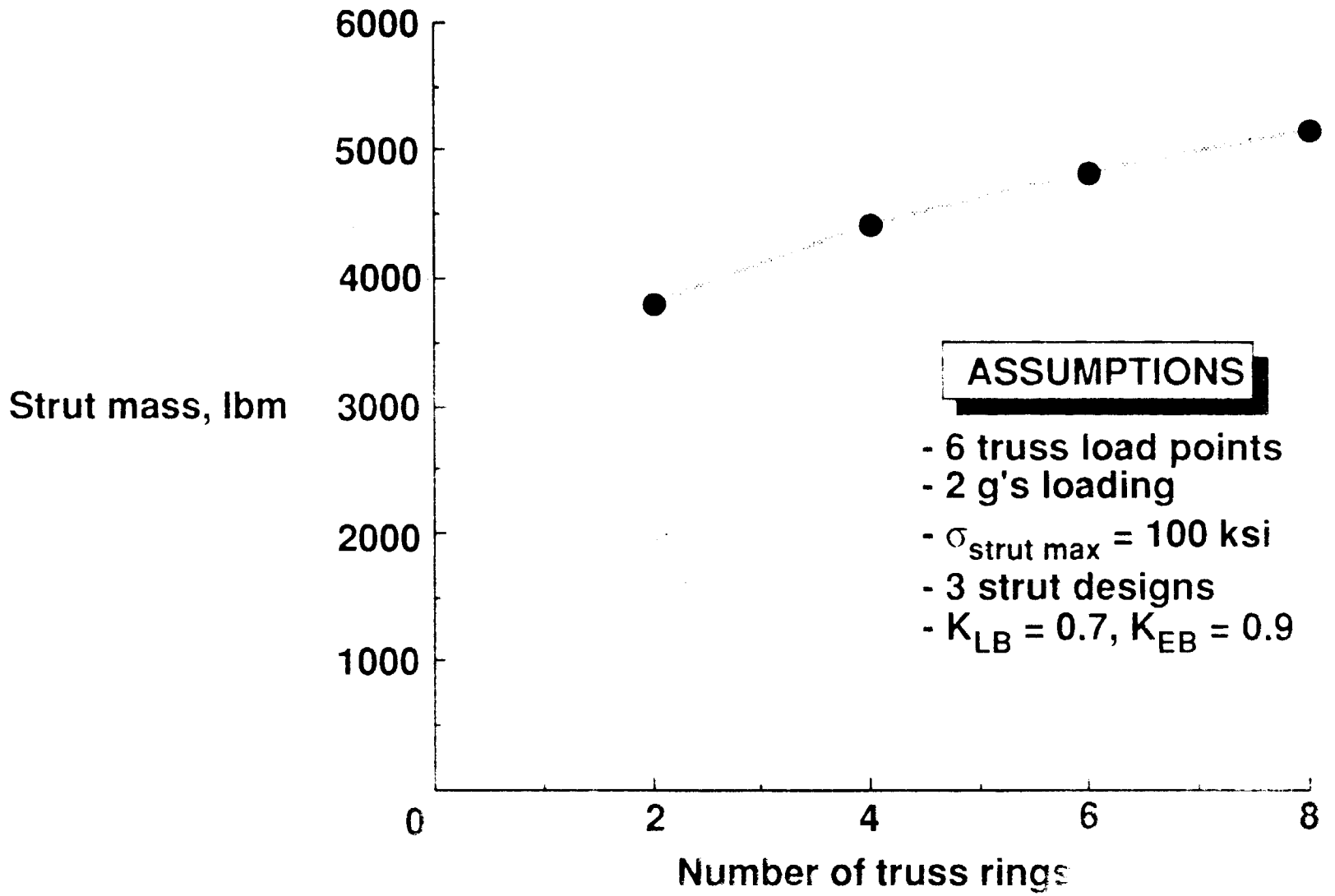

HEX PANEL FACE SHEET THICKNESS FOR MINIMUM MASS

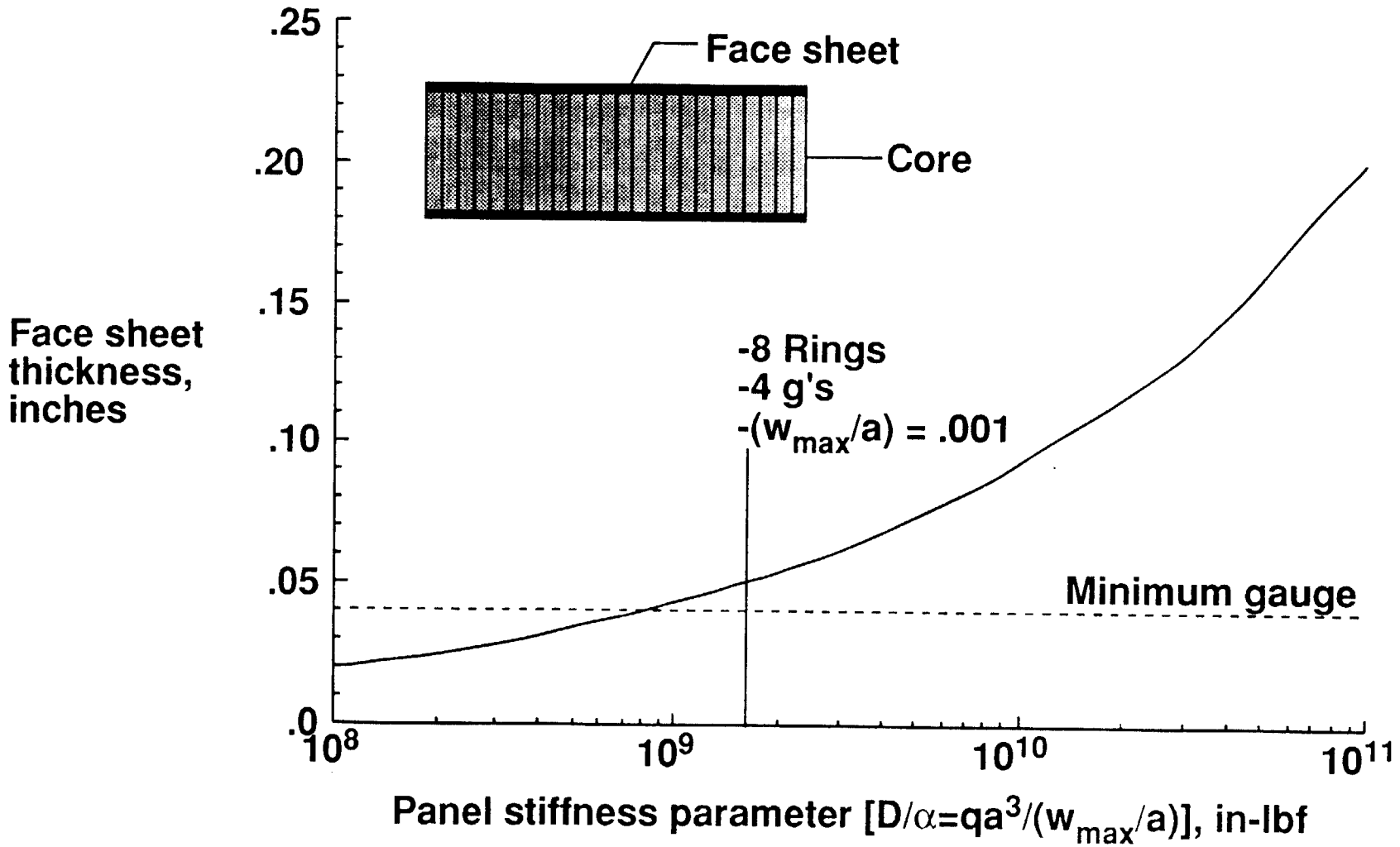

Figure 19.

NASA

Dorsey 4/6/89

HEX PANEL CORE THICKNESS FOR MINIMUM MASS

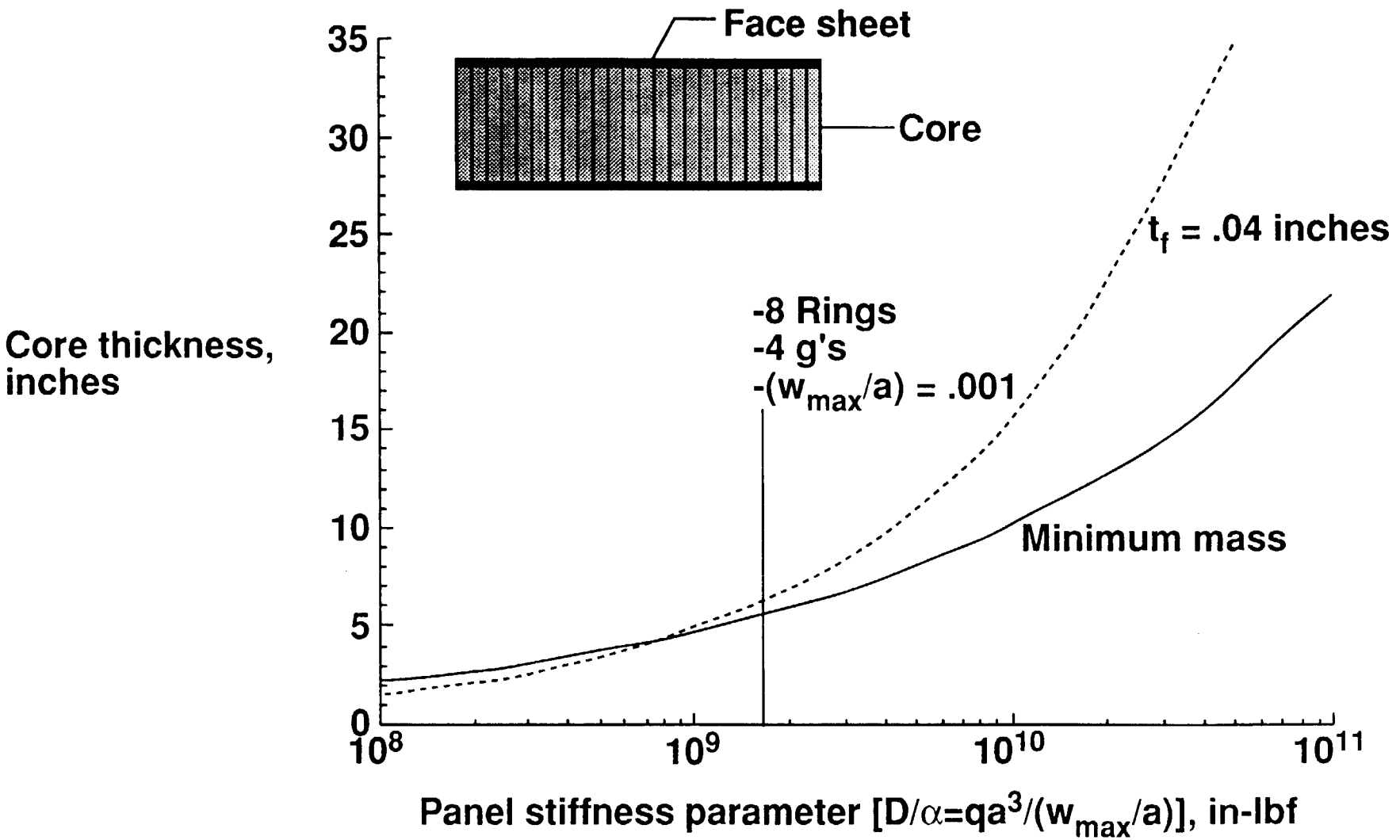

Figure 20.

NASA

Dorsey 4/5/89

AEROBRAKE HEX PANEL MASS

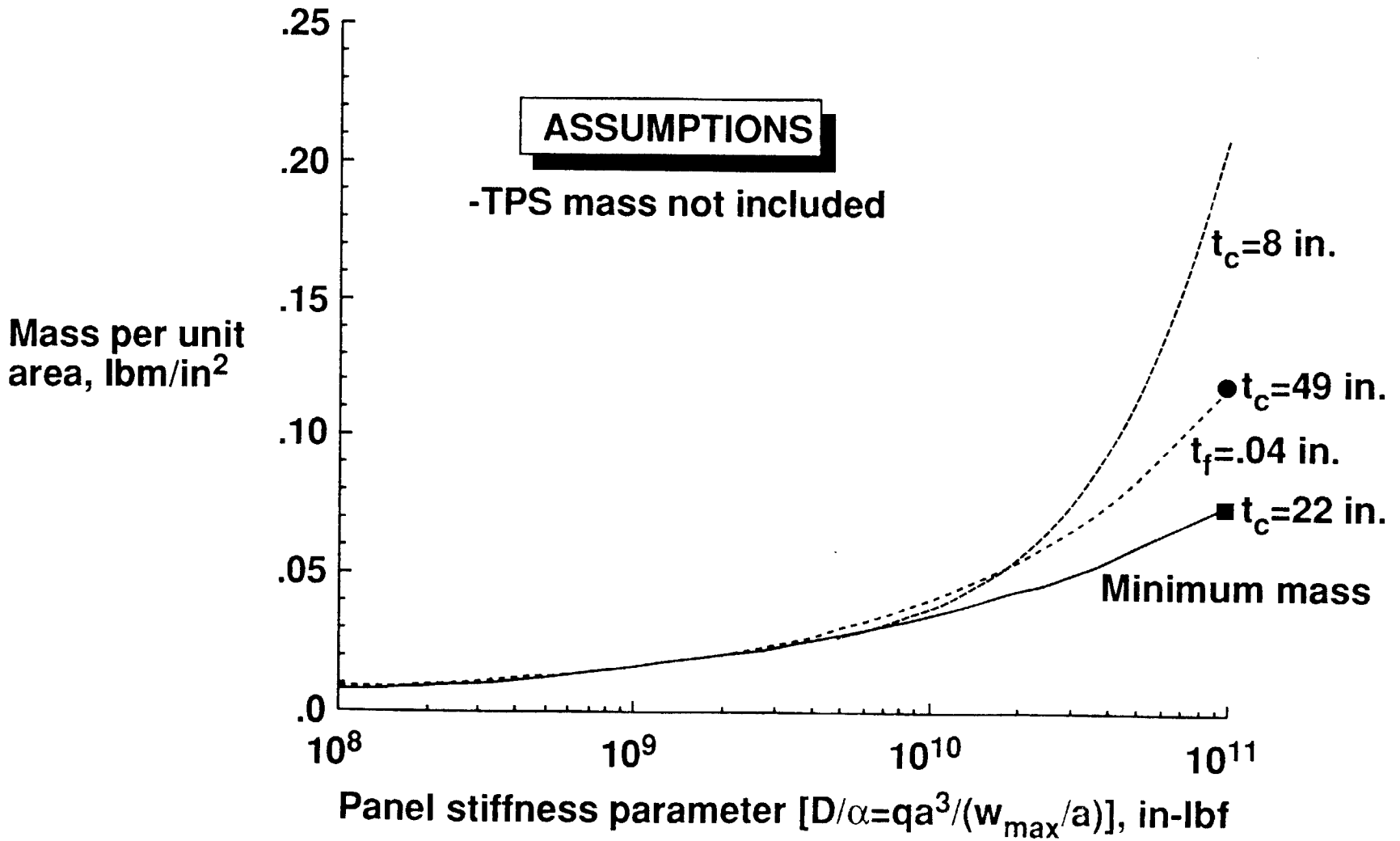

Figure 21.

NASA

Dorsey 4/6/89

HEATSHIELD PANEL DEFLECTION PROFILE DUE TO UNIFORM PRESSURE LOADING

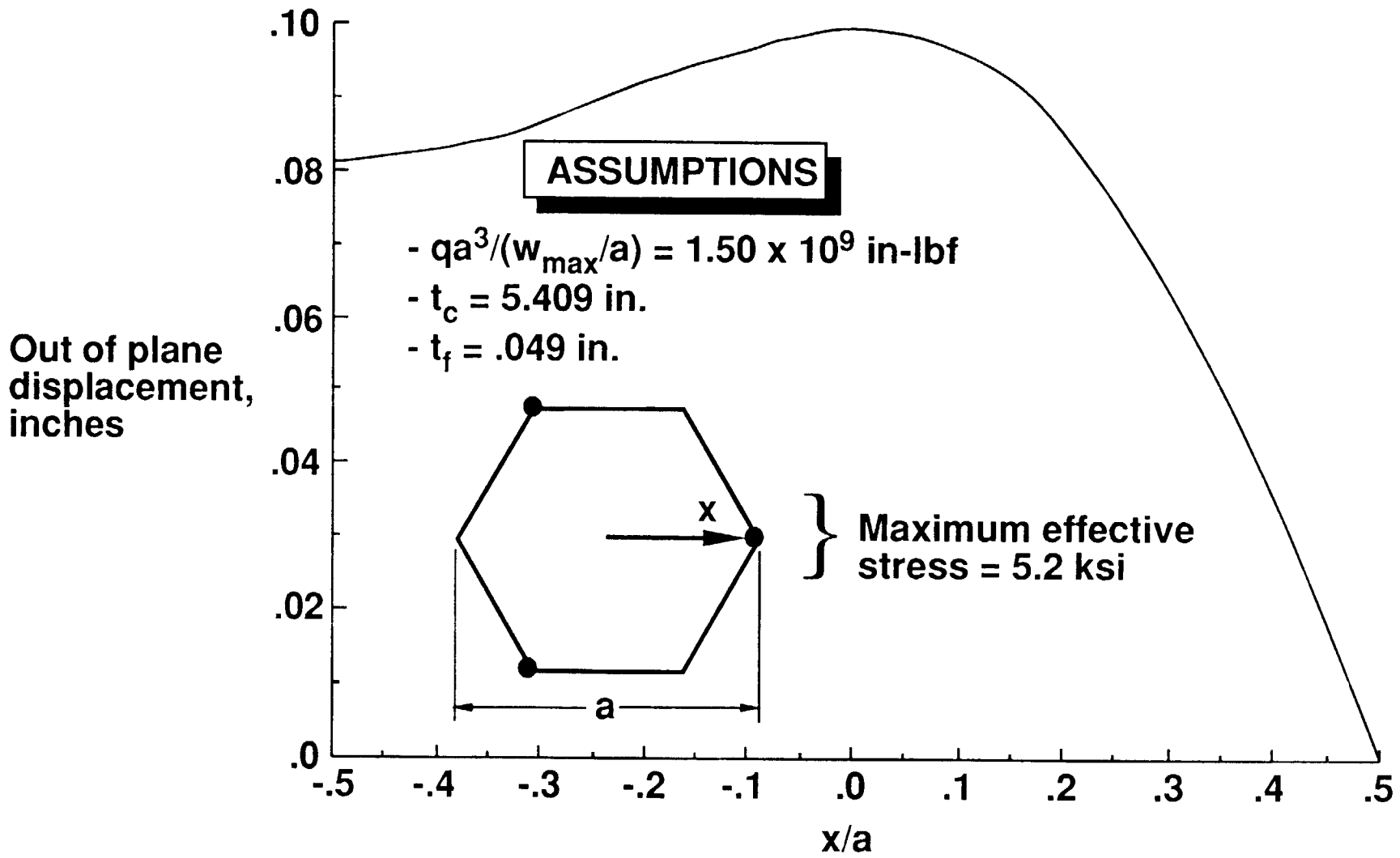

Figure 22.

NASA

Dorsey 4/12/89

MASS FOR 120 FOOT DIAMETER AEROBRAKE

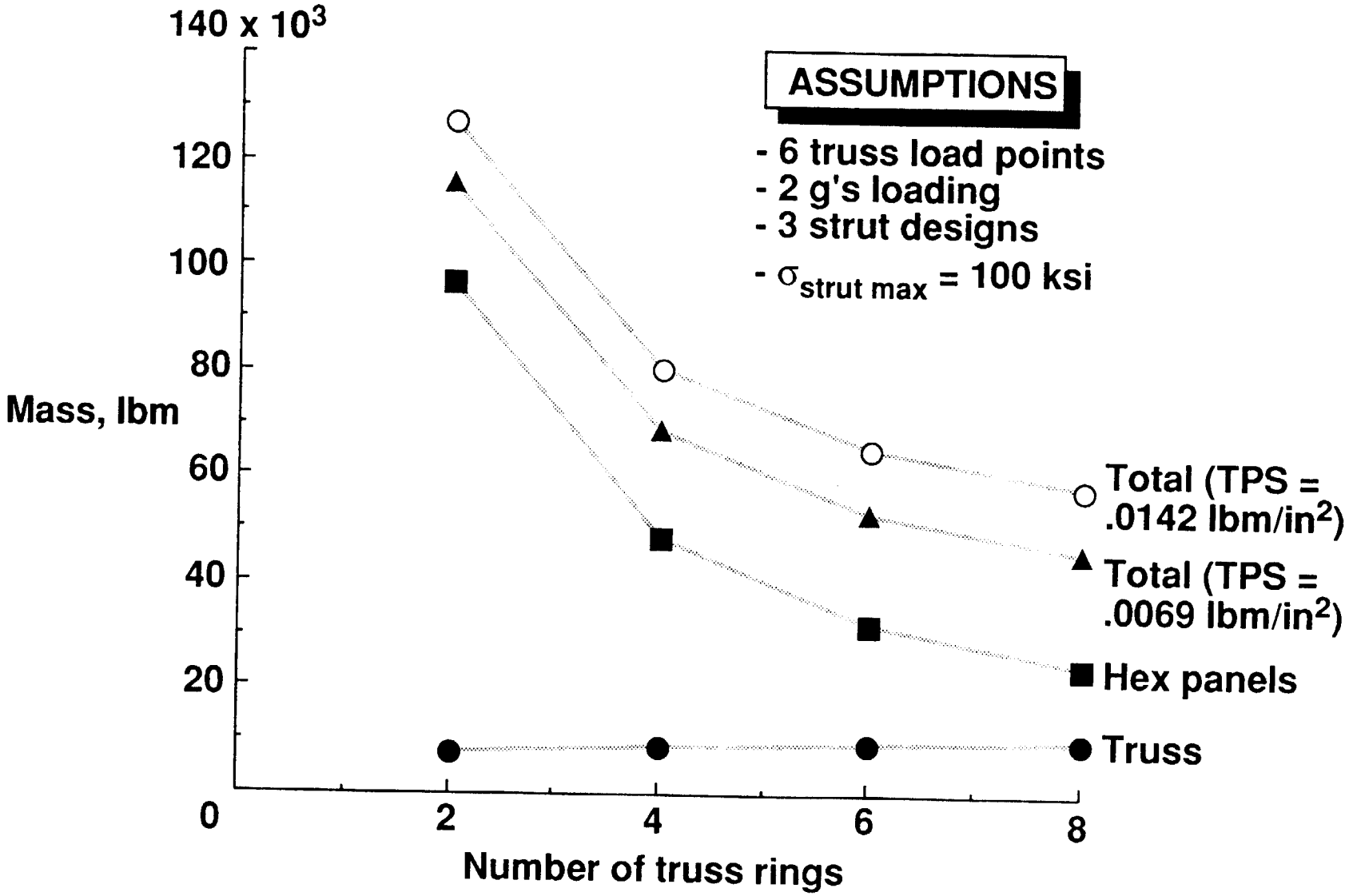

Figure 23.

NASA

INCREASING DECELERATION INCREASES AEROBRAKE TOTAL MASS

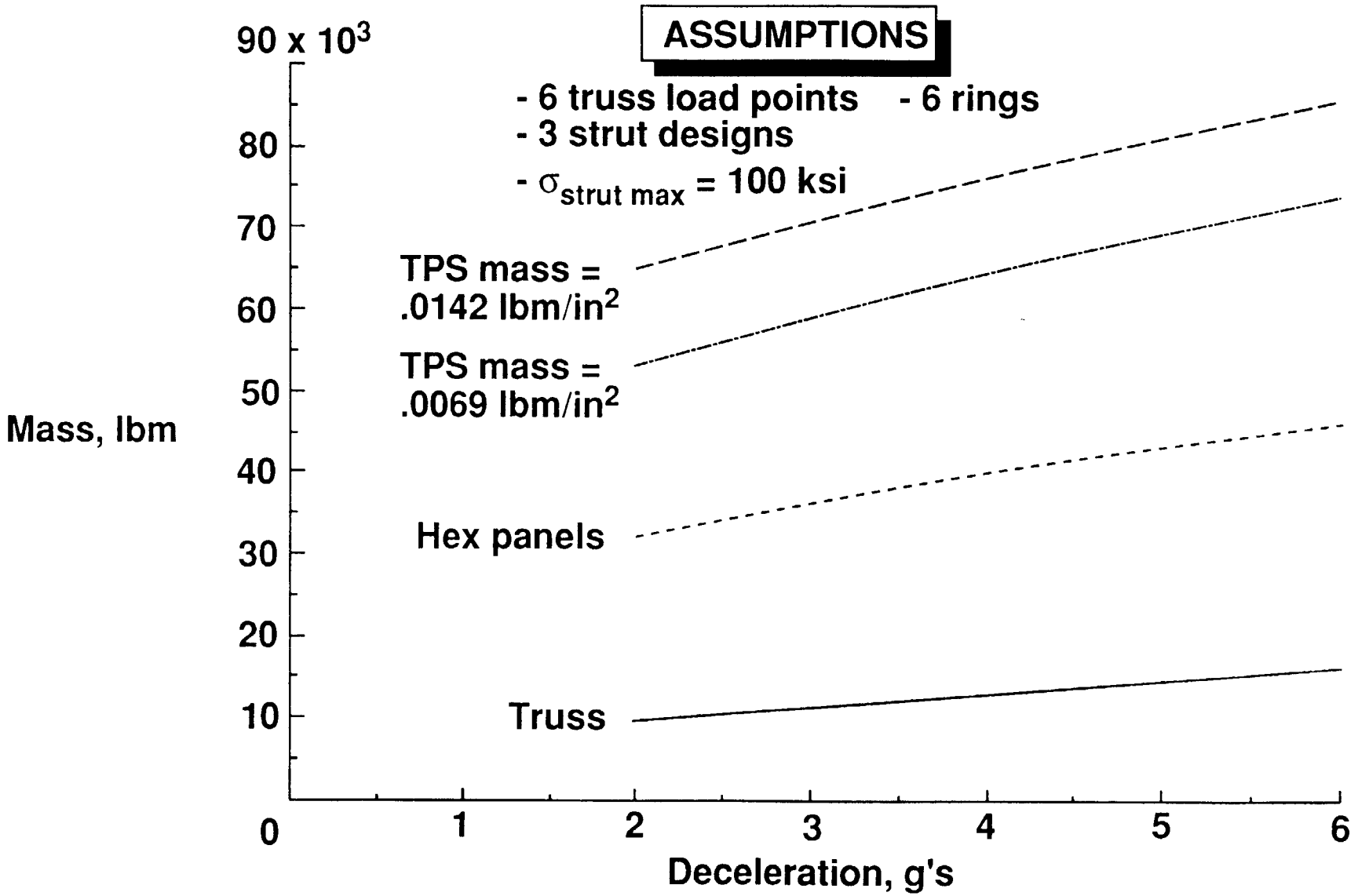

Figure 24.

NASA

Dorsey 6/26/89

PACKAGING VOLUME FOR 120 FOOT DIAMETER AEROBRAKE

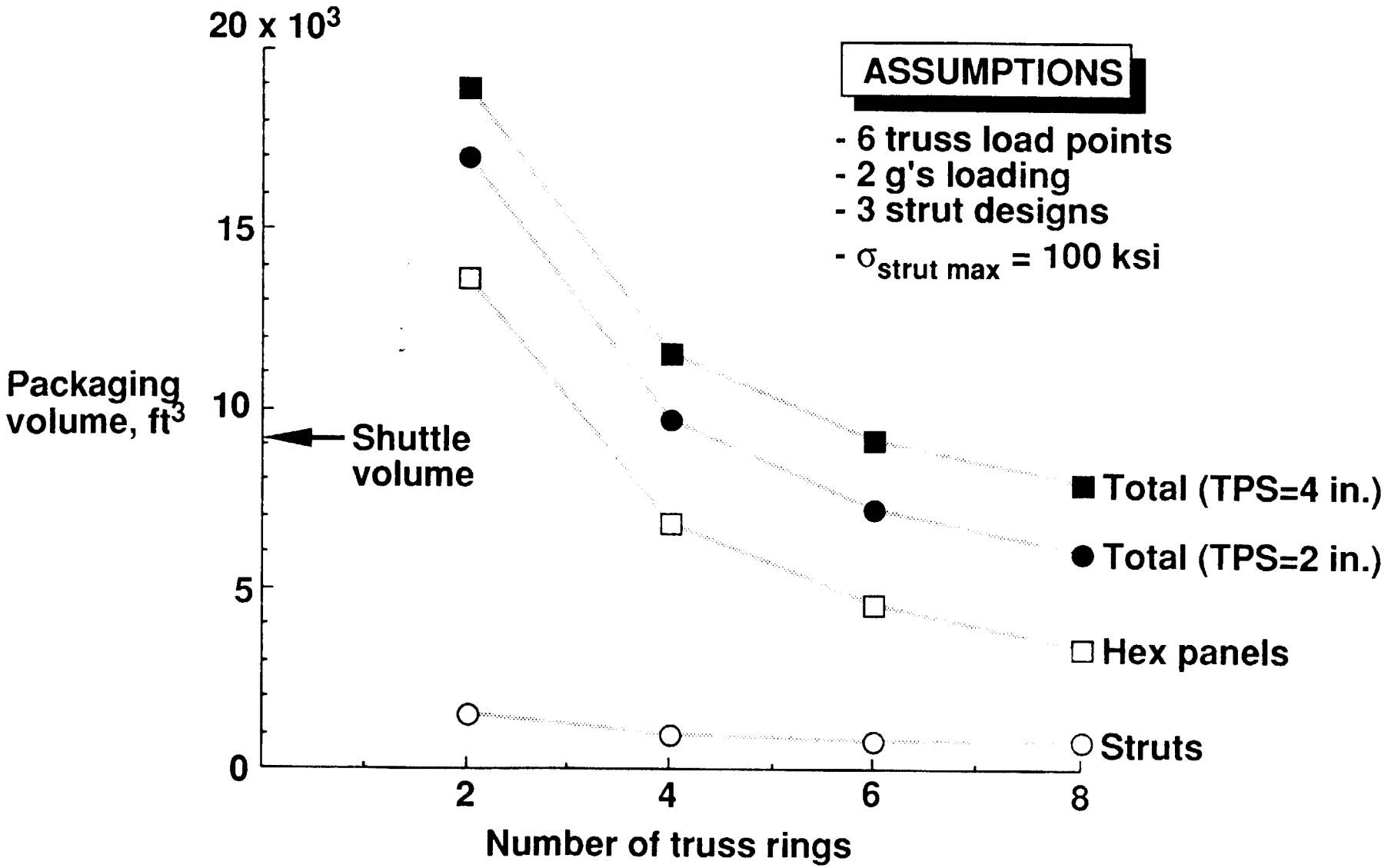

Figure 25.

NASA

Dorsey 6/26/89

AEROBRAKE STRUT & PANEL PART COUNTS

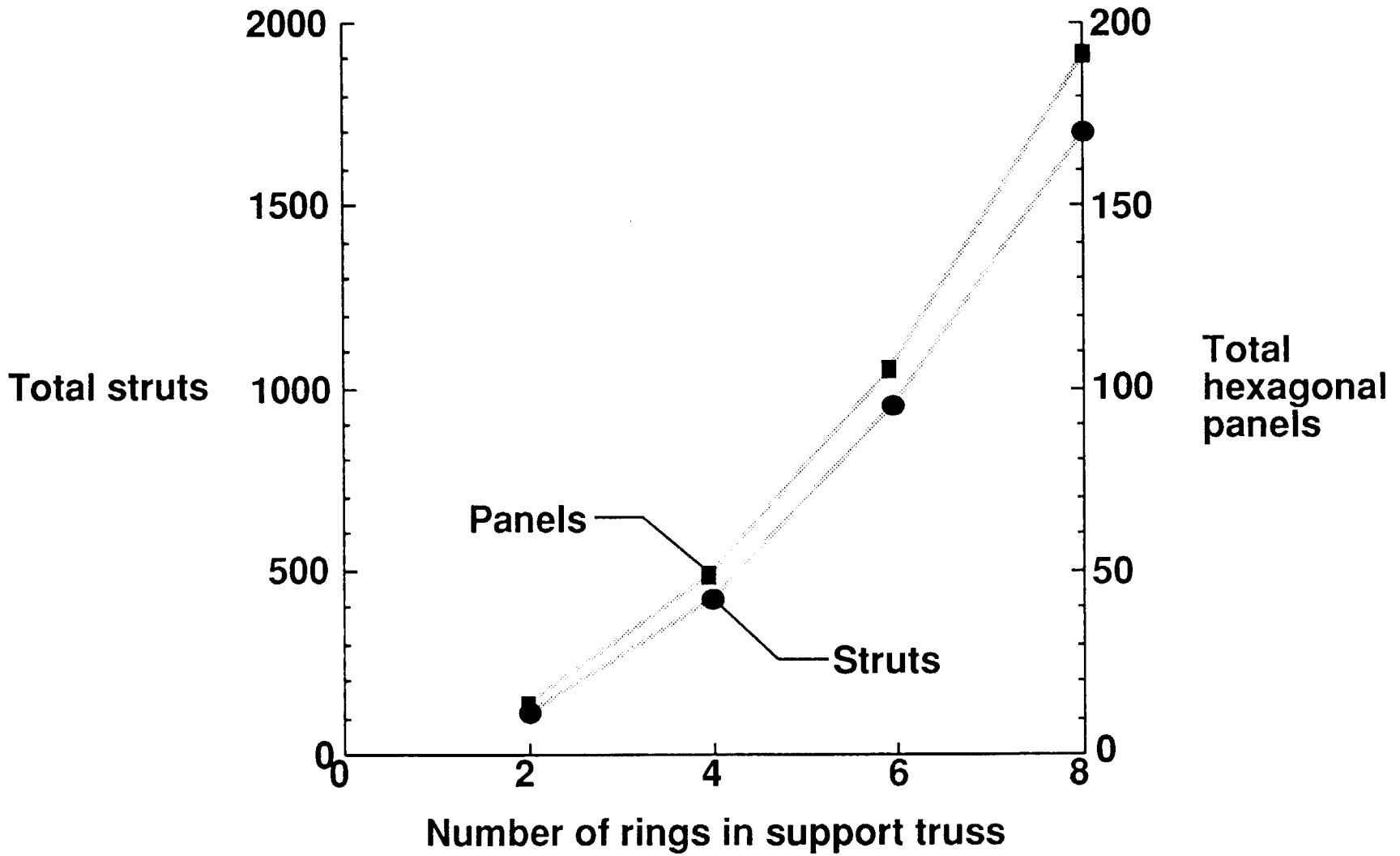

Figure 26.

NASA

Dorsey 7/26/89

CURVATURE EFFECTS ON AEROBRAKE PERFORMANCE

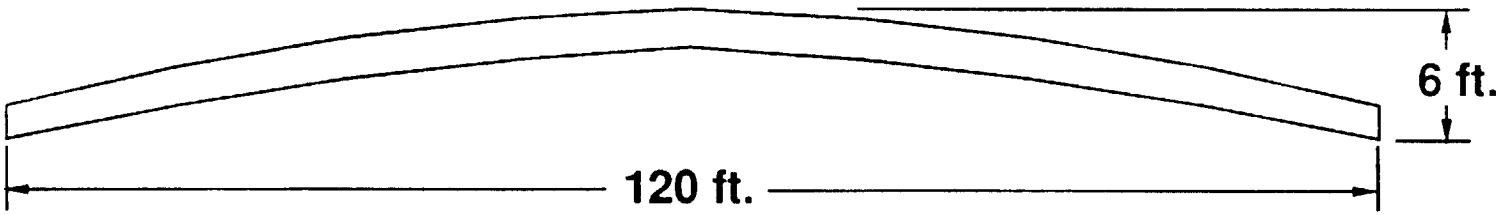

Aerobrake L/D = 0.5

TRUSS

Δ Maximum Deflection = -10%

Δ Maximum Strut Load = -2%

Δ Truss Mass = -.6%

HEATSHIELD PANEL

Δ Maximum Deflection = -16%

Δ Panel Mass = +.8%

NASA

Figure A1.

Dorsey 4/12/89

NASA

Report Documentation Page

1. Report No.	2. Government Accession No.	3. Recipient's Catalog No.
NASA TM-101612		

4. Title and Subtitle	5. Report Date
Preliminary Design of a Large Tetrahedral Truss/ Hexagonal Heatshield Panel Aerobrake	September 1989
	6. Performing Organization Code

7. Author(s)	8. Performing Organization Report No
John T. Dorsey and Martin M. Mikulas, Jr.	
	10. Work Unit No
	591-22-21-01
9. Performing Organization Name and Address	11. Contract or Grant No.
Langley Research Center Hampton, VA 23665-5225	
	13. Type of Report and Period Covered
12. Sponsoring Agency Name and Address	Technical Memorandum
National Aeronautics and Space Administration Washington, DC 20546-0001	14. Sponsoring Agency Code

15. Supplementary Notes

16. Abstract

This paper introduces an aerobrake structural concept consisting of two primary components: 1) a lightweight erectable tetrahedral support truss, and 2) sandwich hexagonal heatshield panels which, when attached to the truss, form a continuous impermeable aerobraking surface. Generic finite element models and a general analysis procedure to design tetrahedral truss/hexagonal heatshield panel aerobrakes is developed, and values of the aerobrake design parameters which minimize mass and packaging volume for a 120-foot-diameter aerobrake are determined. Sensitivity of the aerobrake design to variations in design parameters is also assessed. The results show that a 120-foot-diameter aerobrake is viable using the concept presented in this paper (i.e., the aerobrake mass is less than or equal to 15 percent of the payload spacecraft mass). Minimizing the aerobrake mass (by increasing the number of rings in the support truss) however, leads to aerobrakes with the highest part count.

17. Key Words (Suggested by Author(s))	18. Distribution Statement
Large space structures Space truss Aerobrake Structural design	Unclassified - Unlimited Subject category - 18

19. Security Classif. (of this report)	20. Security Classif. (of this page)	21. No. of pages	22. Price
Unclassified	Unclassified	45	A03

NASA FORM 1626 OCT 86